AD NUMBER: AD0809387

LIMITATION CHANGES

TO:

Approved for public release; distribution is unlimited.

FROM:

Distribution authorized to U.S. Government agencies and their contractors; Export Controlled; 2 Feb 1967. Other requests shall be referred to Air Force Materials Laboratory, Wright-Patterson AFB, OH 45433.

AUTHORITY

AFML ltr dtd 29 Mar 1972

AFM-TR-66-89
Part II

ELEVATED TEMPERATURE DUCTILITY MINIMA AND CREEP STRENGTHENING OF COATED AND UNCOATED COLUMBIUM ALLOYS

B. C. Allen, E. S. Bartlett, and B. A. Wilcox

Battelle Memorial Institute

TECHNICAL REPORT AFML-TR-66-89, Part II

February 1967

Air Force Materials Laboratory
Research and Technology Division
Air Force Systems Command
Wright-Patterson Air Force Base, Ohio

AFML-TR-66-89
Part II

ELEVATED TEMPERATURE DUCTILITY MINIMA AND CREEP STRENGTHENING OF COATED AND UNCOATED COLUMBIUM ALLOYS

B. C. Allen, E. S. Bartlett, and B. A. Wilcox

Battelle Memorial Institute

FOREWORD

This report was prepared by Battelle Memorial Institute, under United States Air Force Contract Number AF33(615)-1727. This contract was initiated under Project Number 7351, "Metallic Materials", Task Number 735101, "Refractory Metals."

The project was administered under the direction of the Air Force Materials Laboratory, Research and Technology Division, with Mr. Larry D. Parsons as acting project engineer.

This report covers the period from 1 September 1965 to 30 August 1966.

The manuscript of this report was released by the authors December 1966 for publication.

This technical report has been reviewed and is approved.

I. PERLMUTTER
Chief, Metals Branch
Metals and Ceramics Division
AF Materials Laboratory

ABSTRACT

In Phase 1 an investigation was made of factors affecting the tensile ductility minimum behavior of coated columbium alloys in air in the intermediate temperature range 700-1100 C. In the case of TRW Cr-Ti-Si coated Cb-10W and Cb-10W-2.5Zr (Cb-752 Alloy), contamination and embrittlement by air at the base of coating cracks is the major factor responsible for loss of ductility. Apparent mechanical interaction between coating and substrate plays a smaller role, but becomes more important with decreasing substrate thickness. The presence of zirconium and dynamic strengthening of the substrate have relatively little effect on ductility.

A study of dynamic strengthening during creep of Cb-10W-2.5Zr and Cb-10W was the objective of Phase 2. All creep testing was done in a vacuum of ~10^{-6} torr and under constant stress conditions. The temperature range of interest was ~800-1200 C. In long-time creep tests, the usual dynamic strengthening process in the Cb-10W-2.5Zr alloy was complicated by additional hardening due to internal oxidation. The Cb-10W-2.5Zr alloy was considerably stronger in creep than Cb-10W. The possible strengthening effects of Zr are discussed.

TABLE OF CONTENTS

TABLE OF CONTENTS
(Continued)

LIST OF ILLUSTRATIONS

LIST OF ILLUSTRATIONS
(Continued)

LIST OF TABLES

PHASE 1. TENSILE DUCTILITY MINIMUM IN COATED AND UNCOATED COLUMBIUM ALLOYS

INTRODUCTION

A pronounced minimim occurs in the tensile[1, 2]* and bend ductility[3] of coated columbium alloys tested in air at intermediate temperatures of about 700-1100 C (0.35-0.50 of the melting point). For example, reductions in area of 40-90 percent for uncoated alloys tested in vacuum sometimes drop to near zero when the coated alloys are strained in air.

The objective of this phase of the program was to determine the mechanisms responsible for the embrittlement of coated columbium-base alloys in the temperature range 700-1100 C. Experiments were designed to evaluate the importance of the following factors on tensile ductility:

(1) Zirconium content of substrate

(2) Dynamic strengthening of substrate

(3) Environment

(4) Mechanical interaction between substrate and coating.

Cb-10W** and the commercial alloy Cb-752 (Cb-10W-2.5Zr) were used as substrates, and the coatings used were TRW Cr-Ti-Si and Sylcor Ag-Si-Al-Mo.

MATERIALS

Substrate

Thirty-mil-thick Cb-10W and Cb-752 and 120-mil Cb-752 sheets were supplied by the Stellite Division of Union Carbide Corporation.

Cb-10W

Cb-10W sheet was prepared from a 15-pound 4-inch-diameter electron-beam-melted ingot. The latter was cut in two pieces, coated with borosilicate glass for oxidation protection and lubrication, and press forged at 1200 C. After being machined and

*References are given on page 54.

**Unless otherwise specified, alloy compositions are given in weight percent.

vacuum annealed at 1540 C, the pieces were warm rolled at ~350 C to 0.160 inch. Following a 1-hour vacuum anneal at 1540 C, the alloy was cold rolled in the same direction to ~80 percent reduction in area to 30-mil sheet. The chemistry of the ingot and finished sheet are given in Table 1.

Recrystallization to an average grain size of 0.073 mm was done by vacuum annealing 1 hour at 1620 C. The structure after a simulated coating thermal treatment appeared as shown in Figure 1a. Since columbium and tungsten form a continuous series of bcc solid solutions[4], the fine precipitates undoubtedly are the result of interstitial impurities.

Cb-752

Cb-752 sheet was prepared from part of a 250-pound electron-beam-melted ingot measuring 27-3/16 x 10-1/2 x 2-9/16 inches. Following vacuum annealing at 1540 C, the alloy was hot rolled at 1200 C in a protective can to 0.680 inch. Following a similar vacuum anneal, the alloy was warm rolled at ~350 C in the same direction to give 120-mil sheet with a reduction of ~80 percent. After a vacuum anneal at 1430 C, some of the sheet was cold rolled in the same direction to 30 mils, thereby giving a cold reduction of ~75 percent. The chemistry of the ingot and sheet are given in Table 1.

Recrystallization in vacuum for 1 hour at 1540 C resulted in an average grain size of 0.057 mm for the 30 mil and 0.037 mm for the thicker sheet. The difference probably was caused by the more severe cold work in the 30-mil sheet. The typical structure is shown in Figure 1b. Aligned parallel to the rolling direction is a fine dispersion, identified by X-ray diffraction to be (Cb, Zr), C, monoclinic ZrO_2, and/or fcc ZrO_2.[6]

Coating

TRW Cr-Ti-Si

The coating examined most extensively was the TRW Cr-Ti-Si type applied in a 2-cycle vacuum deposition process from an activated pack. In the first cycle, the specimens were packed in minus 8, plus 30 mesh 60Cr-40Ti alloy powder with 0.5 percent KF activator. The assembly was enclosed in a carbon retort and heated for 8 hours at 1260 C at 10^{-2} mm. The silicon was similarly applied by heating minus 8, plus 30 mesh powder with 1 percent KF for 4 hours at 1120 C.

According to Figures 2a and 3, the resulting coating on Cb-752 and Cb-10W consisted of metal disilicides with minor amounts of subsilicides and/or Laves phases $(Cb, Ti)Cr_2$ totalling 2.4 ± 0.4 mils thick. The phases were identified from metallography and concentration profiles[7] of a similar alloy (D-43) shown in Figure 4. The outer layers consisted of a Cr, Ti rich disilicide and a Cb-rich disilicide. Below these was a white phase, $(Cb, Ti)Cr_2$, which tended to penetrate substrate grain boundaries. Adjacent to the coating, the substrate had a 0.5-mil zone containing dissolved Cr, Ti, and Si. Although not identified metallographically, traces of subsilicide were also probably present. Because of tensile stresses generated by differential thermal contraction (see

TABLE 1. ANALYSES OF Cb-10W AND Cb-752

Form	Final Vacuum Heat Treatment[a]	Weight Percent		Ppm by Weight						
		W	Zr	Mo	Ni	Ta	C	O	N	H
		Cb-10W								
Electron-beam-melted ingot	None	9.92	--	--	--	--	10	270	115	3
30-mil sheet	None	--	<0.003	50	30	<1000	20	270	103	3
		Cb-752								
Electron-beam-melted ingot	None	9.92	2.85	--	--	--	11	39	65	5
230-mil sheet	None	10.3	3.18	--	--	--	60	47	84	10
120-mil sheet	A	--	--	--	--	--	10	29	25	1
120-mil sheet	B	--	--	--	--	--	10	29	34	1
30-mil sheet	B	--	--	50	30	<1000	20	59	30	1

(a) A = 1 hr 1540 C
B = 1 hr 1540 C + 8 hr 1250 C + 4 hr 1120 C.

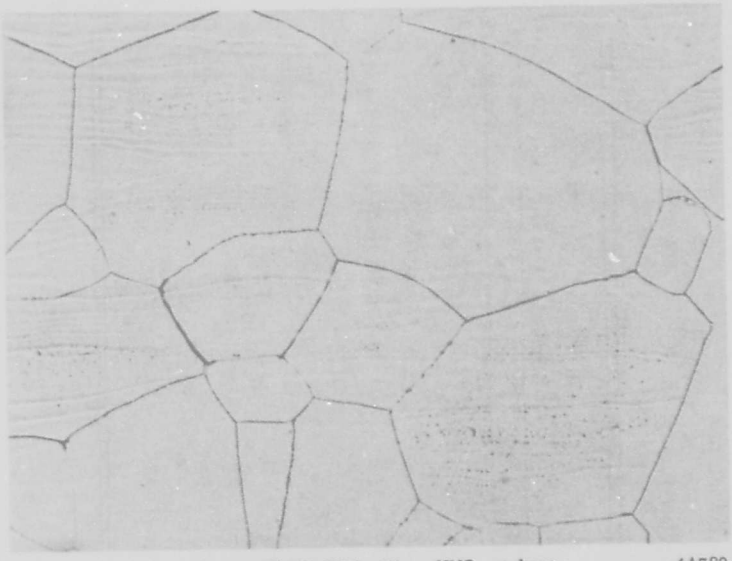

250X 100 cc 20% NH_4FHF + 50 cc HNO_3 etchant 4A789

a. Cb-10W, 1 hr 1620 C + 8 hr 1260 C + 4 hr 1120 C

250X 50 lactic acid, 30 HNO_3, 1 HF etchant N29579

b. Cb-10W-2.5Zr, 1 hr 1540 C + 8 hr 1260 C + 4 hr 1120 C

FIGURE 1. LONGITUDINAL MICROSTRUCTURES OF 30-MIL Cb-10W AND Cb-752 SHEET AFTER VACUUM ANNEALING

500X a. As Coated OA051

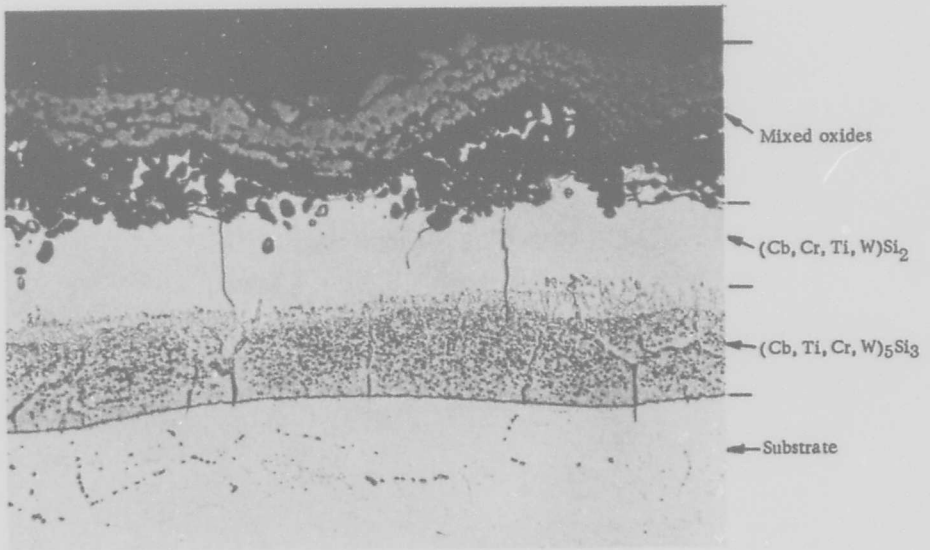

500X b. As Coated and Air Annealed 50 Hr 1370 C OA054

FIGURE 2. MICROSTRUCTURES OF Cr-Ti-Si COATED Cb-752 SHEET

Phases identified from Figure 4.
50 lactic acid - 30 HNO_3 - 1 HF etchant.

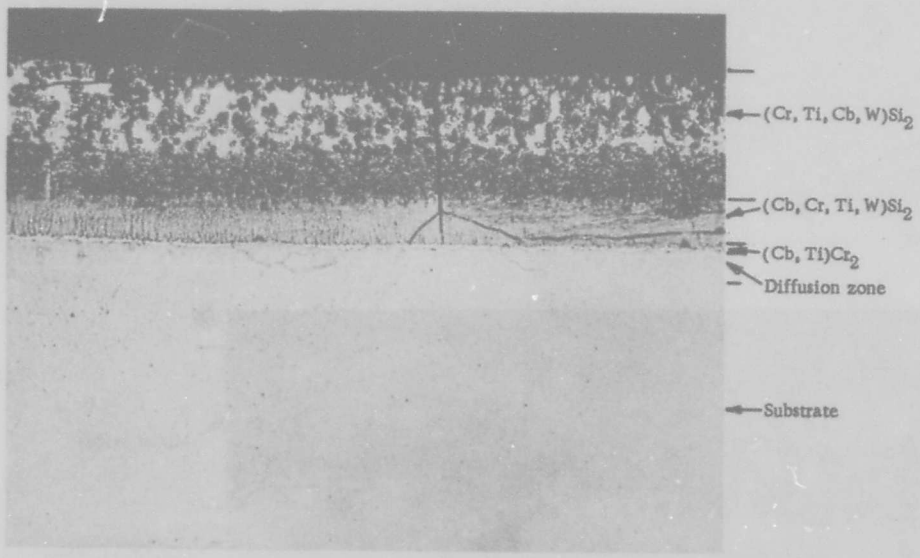

500X 50 lactic acid – 30 HNR_3 – 2 HF etchant 6A529

FIGURE 3. MICROSTRUCTURE OF Cr-Ti-Si COATED Cb-10W SHEET

Phases identified from Figure 4.

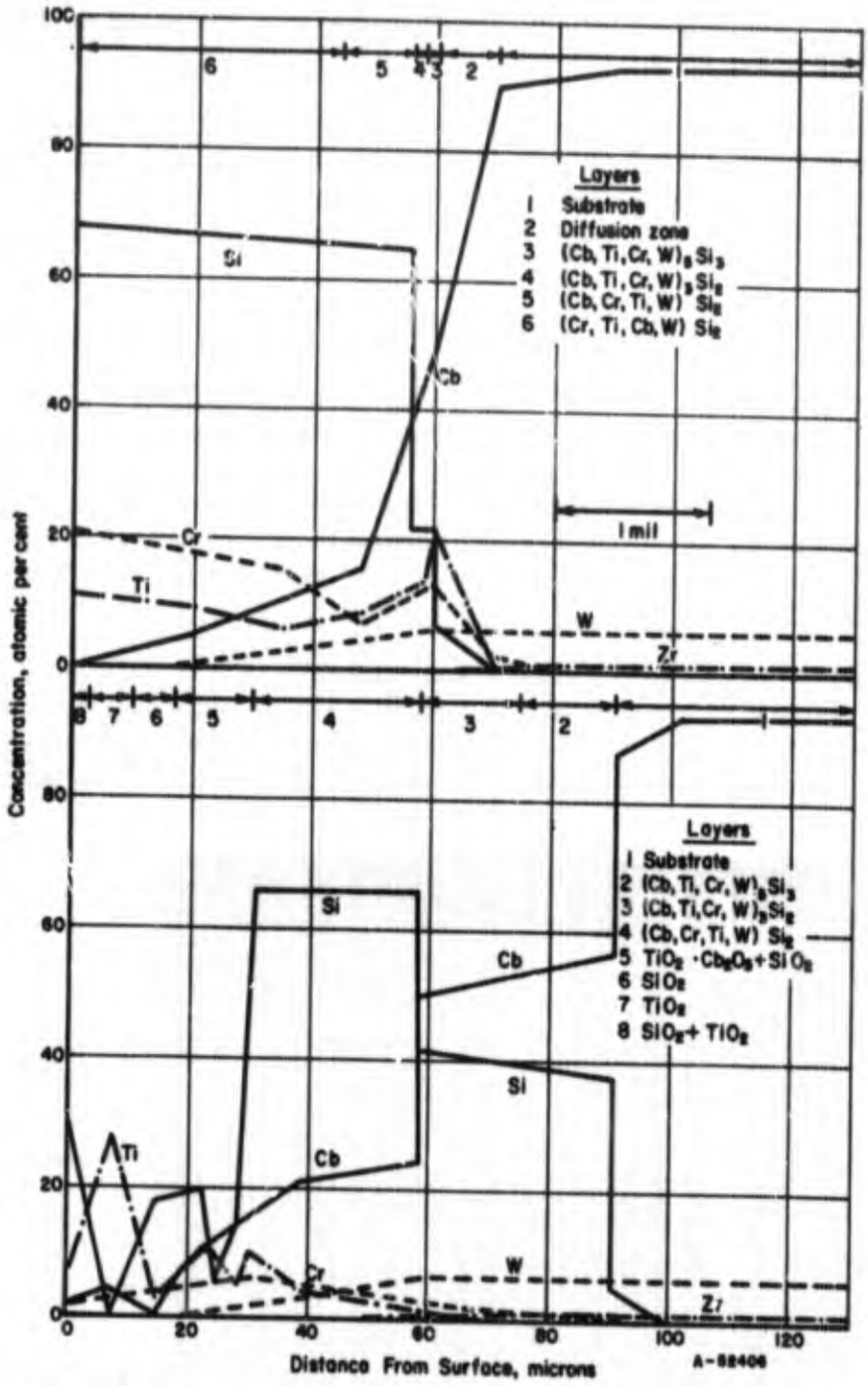

FIGURE 4. CONCENTRATION PROFILE OF Cb-10W-1Zr-0.1C(D-43 Alloy) COATED WITH Cr-Ti Si[7]

Top: as coated
Bottom: coated and annealed 50 hours at 1370 C in air at 1 atmosphere.

Appendix A) many cracks appeared in the coating on cooling to room temperature and resulted in a mosaic pattern having blocks about 5 mils in diameter. Characteristically, the Cr-Ti-Si coating is hard [~1000 DPH[8]] and brittle compared to ~185 DPH for recrystallized Cb-752.

For selected studies some of the disilicides were converted to subsilicides by air annealing 50 hours at 1370 C as indicated in Figure 2b. In addition, the Laves phase and diffusion zone were essentially eliminated. In this condition the coating still had adequate oxidation resistance for static tests in air.[7]

Sylcor Ag-Si-Al-Mo

The other coating used was the R508 Ag-Si-Al-Mo coating supplied by the Sylcor Division of General Telephone and Electronics Corporation. The coating was applied in a two-step slurry process, done by spraying the metal powders blended in a lacquer vehicle followed by a short-time (<1 hour) diffusion treatment in argon at 1260 C.[9] The resulting coating was ~6 mils thick, composed of a 2-mil disilicide zone overlaid with a 4-mil low-melting (750-800 C) metal reservoir capable of filling cracks in the disilicide layer.

An electron microprobe analysis made on Ag-Si-Al-Mo coated Cb-752 was in essential agreement with a similar analysis[9] made on unalloyed columbium. As indicated in Figure 5, the outer layer consisted of a silver-aluminum alloy matrix [containing about 18 atomic percent aluminum[9]] plus minor amounts of Cb and Mo. Included

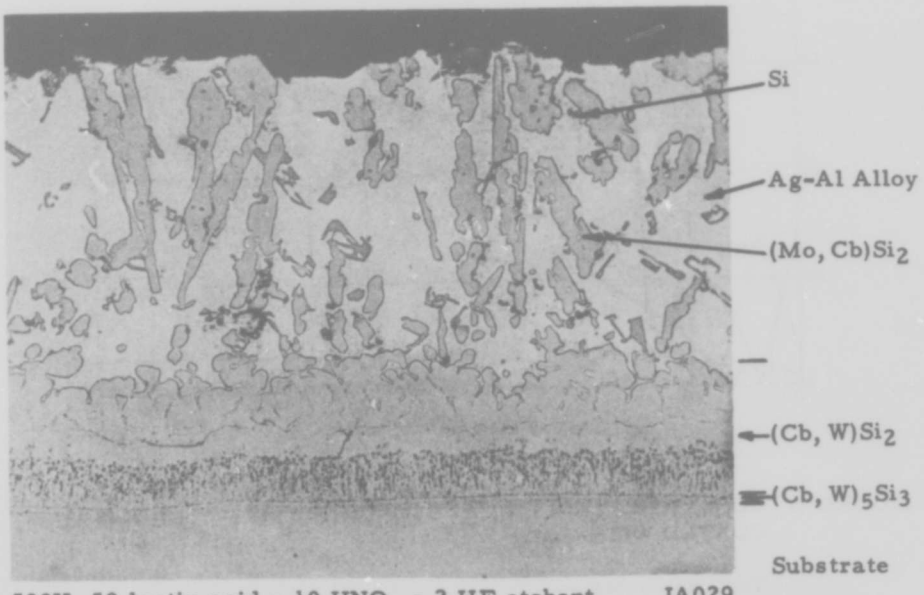

500X 50 lactic acid - 10 HNO_3 - 2 HF etchant. IA029

FIGURE 5. MICROSTRUCTURE OF Ag-Si-Al-Mo COATED Cb-752 SHEET

Phases identified from microprobe analysis and Reference 9.

were large amounts of a light gray phase (Mo, Cb)Si_2 and small amounts of a dark gray free silicon phase. Adjacent to the multiphase layer was a layer consisting of basically (Cb, W)Si_2 with minor variations and contained traces (~1 atomic percent) of aluminum. Adjacent to the substrate were two thin layers of subsilicide $(Cb, W)_5Si_3$, one or both of which contained 1.5 atomic percent iron.

EXPERIMENTAL WORK

Specimen Preparation

Pin-type sheet tensile specimens of Cb-10W and Cb-752 were prepared having a reduced section of 0.25 inch wide and 1 inch long according to Figure 6. The axis was generally parallel to the rolling direction. The pin was the same diameter as the gage width, with the cross-sectional area around the holes being at least twice that of the gage cross section. All corners were generously rounded. The 120-mil sheet was symmetrically surface ground to 100 mils. The 30-mil sheet was uniform to ±1 mil and did not require grinding. Specimens to be Cr-Ti-Si coated were recrystallized 1 hour at 1 x 10^{-5} mm at 1620 C for Cb-10W and at 1540 C for Cb-752. All of the uncoated specimens were similarly recrystallized and further annealed 8 hours at 1260 C plus 4 hours at 1120 C to simulate the thermal history given Cr-Ti-Si coated specimens.

All specimens were abrasive tumbled in silicon carbide at TRW to radius the edges about 5 mils. This treatment either facilitated coating adherence or maintained uniform geometry. Specimen thicknesses were reduced 0.5-1 mil by the treatment. Tumbling was followed by pickling (20 seconds in 20HF-20H_2SO_4-10HNO_3-5OH_2O) and rinsing in water and alcohol. Coatings were applied as described in the preceding section. Six Cr-Ti-Si coated Cb-752 specimens were air annealed 50 hours at 1370 C in a notched Alundum boat to increase the amount of subsilicide present and alter the state of stress in the coating and substrate.

Tensile Tests in Air

Low Strain Rate

Tensile testing in air up to 1200 C at a nominal strain rate of 0.1 per minute was done in a Nichrome resistance furnace mounted on a Baldwin-Southwark hydraulic machine. Pin-type grips, 3/4-inch diameter, and pins were made of solution treated and aged Udimet 700 bar (see Appendix B for chemistry and heat treatment). Expendable tungsten pins were used near 1200 C. Temperatures were measured by a Chromel-Alumel thermocouple loosely wired to the specimen midsection. The end of an Alundum protection tube prevented reaction between the thermocouple bead and coating above 900 C. The maximum temperature gradient along the gage length was estimated to be 10 C. Load-extension curves were recorded autographically.

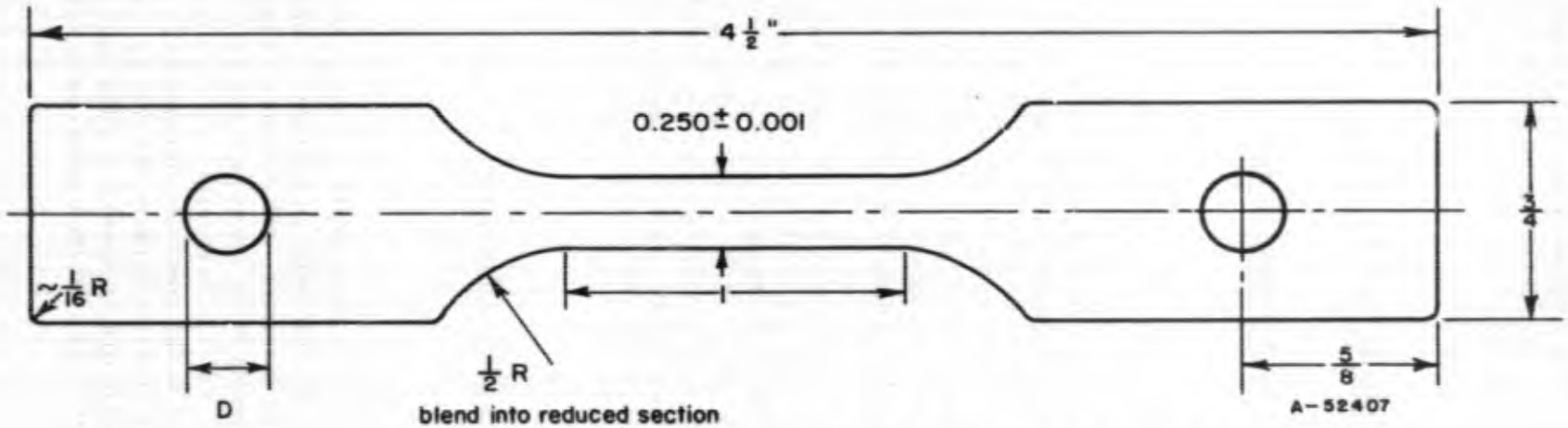

D = 0.255 for uncoated specimens
D = 0.260 for specimens to be coated

FIGURE 6. DESIGN OF SHEET TENSILE SPECIMENS

High Strain Rate

Testing in air at a strain rate of ~100 per minute was done using a Krafft-Hahn dynamic loader equipped with pin-type Udimet 700 grips. The machine operates by expansion of a volume of cold, pressurized gas acting on a driving piston. The machine is hydraulically stiffened by requiring the piston, in addition to loading the specimens, to force a gas-free liquid through a controllable restrictive orifice. Details of operation have been described previously.(10, 11)

Temperatures of 900-1015 C were obtained by induction heating (4-kw spark gap converter, 125-450 kc) a 1-inch-OD Inconel tube susceptor concentric with the specimen axis. Temperatures were measured optically to ±10 C by sighting through a hole in the susceptor onto the surface of the Cr-Ti-Si coated specimens. Black-body corrections were negligible (10 C) according to calibration on a dummy specimen with a 65-mil-diameter hole 240 mils deep. This hole geometry is capable of giving essentially black-body conditions at about 1000 C.(12) Lower temperatures were obtained by using heater tapes and were controlled by a thermocouple.

Load-extension curves were generally taken from a Polaroid photograph of an oscilloscope trace. The load signal came from a calibrated strain gage bridge mounted on the draw bar and time from the oscilloscope sweep velocity. Extension was calculated from the cross head speed and time.

Tensile Tests in Vacuum

Vacuum tensile testing up to 1400 C at a strain rate of 0.1 per minute was done in a Brew tantalum resistance furnace mounted on an Instron machine. Pin-type grips were made of TZM molybdenum rod with TZM or tungsten pins. Temperatures were measured with a Chromel-Alumel thermocouple up to 1100 C. At higher temperatures a Pt-Pt10Rh thermocouple was used. Direct contact with coated specimens above 800 C was prevented by a piece of tungsten foil between the bead and specimen. Maximum temperature gradients were estimated at 20 C, and operating vacua were about 1×10^{-5} mm. Broken specimens were allowed to vacuum cool to ~600 C followed by inert gas cooling to under 100 C.

Ductility and Strength Measurements

Gage lengths and cross-sectional areas were measured on all specimens before and after coating and after testing. Total elongations were within 10 mils of those indicated on load-extension curves. These elongations were converted to percent elongation in 1 inch by considering slight deformation experienced in the specimen shoulders. Allowances for geometry and typical strain hardening indicated an "effective gage length" of 1.3 inches at strains up to maximum load, and thereafter 1 inch to fracture.

Small but measurable losses in load-bearing cross-sectional area were experienced by specimens because of rectangularity losses during abrasive tumbling and substrate consumption by the coating. Corrections for the latter, given in Table 2,

were estimated from metallographic examination and composition (see Figures 2-5) of coating phases present. Substrate yield and ultimate tensile strengths were calculated from load divided by the corrected initial substrate cross-sectional areas. Fracture strengths were calculated using estimates of the final substrate cross-sectional areas.

TABLE 2. EFFECT OF VARIOUS TREATMENTS ON THE LOAD-BEARING CROSS-SECTIONAL AREA OF 30- AND 100-MIL Cb-752 AND Cb-10W SHEET TENSILE SPECIMENS

Treatment	Substrate Consumption, mils/side	Area Reduction, percent	
		30-Mil Sheet	100-Mil Sheet
Radiusing edges to 5 mils by abrasive tumbling	--	1.0	0.3
Cr-Ti-Si coating	0.4	2.9	1.1
Cr-Ti-Si coating + annealing 50 hr 1370 C in air	1.0	7.5	2.8
Ag-Si-Al-Mo coating	0.9	6.8	2.5

Reduction in area values were calculated from the initial minus the final composite area, which was then multiplied by 100/(initial substrate cross-sectioned area). In measured cases where the coating was not adherent, the initial coating area was added to the final area. Measured RA values above 20 percent are believed accurate to ±2 percent RA for 100-mill and ±5 percent RA for 30-mil sheet. In less ductile specimens, where failure occurred at maximum load and elongations appeared uniform, the RA was taken equal to the measured percent elongation in 1 inch. This assumption was consistent with measured changes in specimen dimensions.

The strain-hardening exponent, n, was calculated from load-extension data using the relationship $\sigma = K\epsilon^n$, where σ = true stress, ϵ = true strain, and K is a constant for constant temperature and strain rate. Simplification gives the following approximation at low strains,

$$n \sim \frac{\ell\eta\,(1.01\ P_2/P_1)}{0.694}\ , \qquad (1)$$

where P_1 = load at 1 percent elongation and P_2 = load at 2 percent elongation. Although it varies somewhat with strain, n was calculated at low strains so that strain hardening could be compared in specimens of differing ductilities.

RESULTS AND DISCUSSION

In studying the tensile ductility (reduction in area and elongation) of coated and uncoated columbium alloys, the following parameters were varied:

(1) Temperature: 25-1400 C

(2) Substrate composition: (a) Cb-10W, (b) Cb-10W-2.5Zr

(3) Substrate thickness: (a) 30 mils, (b) 100 mils

(4) Coating:

  (a) As-coated Cr-Ti-Si

  (b) As-coated Cr-Ti-Si annealed to grow subsilicides

  (c) As-coated Ag-Si-Al-Mo

  (d) As-coated Ag-Si-Al-Mo annealed in situ.

(5) Environment: (a) air, (b) vacuum, 1 x 10^{-5} mm

(6) Strain rate: (a) 0.1 per minute, (b) 100 per minute.

Several parameters were held essentially constant. Although some variation existed, the recrystallized grain size of both alloys was ~0.05 mm. Thermal histories of coated and uncoated specimens were the same. Uncoated specimens and specimens to be Ag-Si-Al-Mo coated were given the TRW Cr-Ti-Si coating thermal treatment of 8 hours at 1260 C plus 4 hours at 1120 C in vacuum. The diffusion anneal for the Ag-Si-Al-Mo coating process is expected to have had little additional effect. Generally the tensile axis was parallel to the sheet rolling direction. In some cases, transverse specimens of 100-mil Cb-752 sheet were used. Since no significant difference was found between room-temperature longitudinal and transverse tensile properties, possible anisotropy effects were neglected. Except for thickness, the geometries of all specimens were the same.

Uncoated Cb-752

Tensile properties of uncoated 30- and 100-mil Cb-752 sheet are given in Figure 7 and Tables 7 and 8 (Appendix C) as a function of temperature. With increasing temperatures up to 600 C, there is a steady drop in strength and little change in ductility. At 600-950 C, dynamic strengthening is indicated by serrated yielding, a strength maximum, and increased strain hardening. The temperature range is in agreement with the 500-1000 C range found by Chang for Cb-1Zr.[13] A mild loss in elongation appears to be associated with dynamic strengthening, but reduction in area remains unaffected.

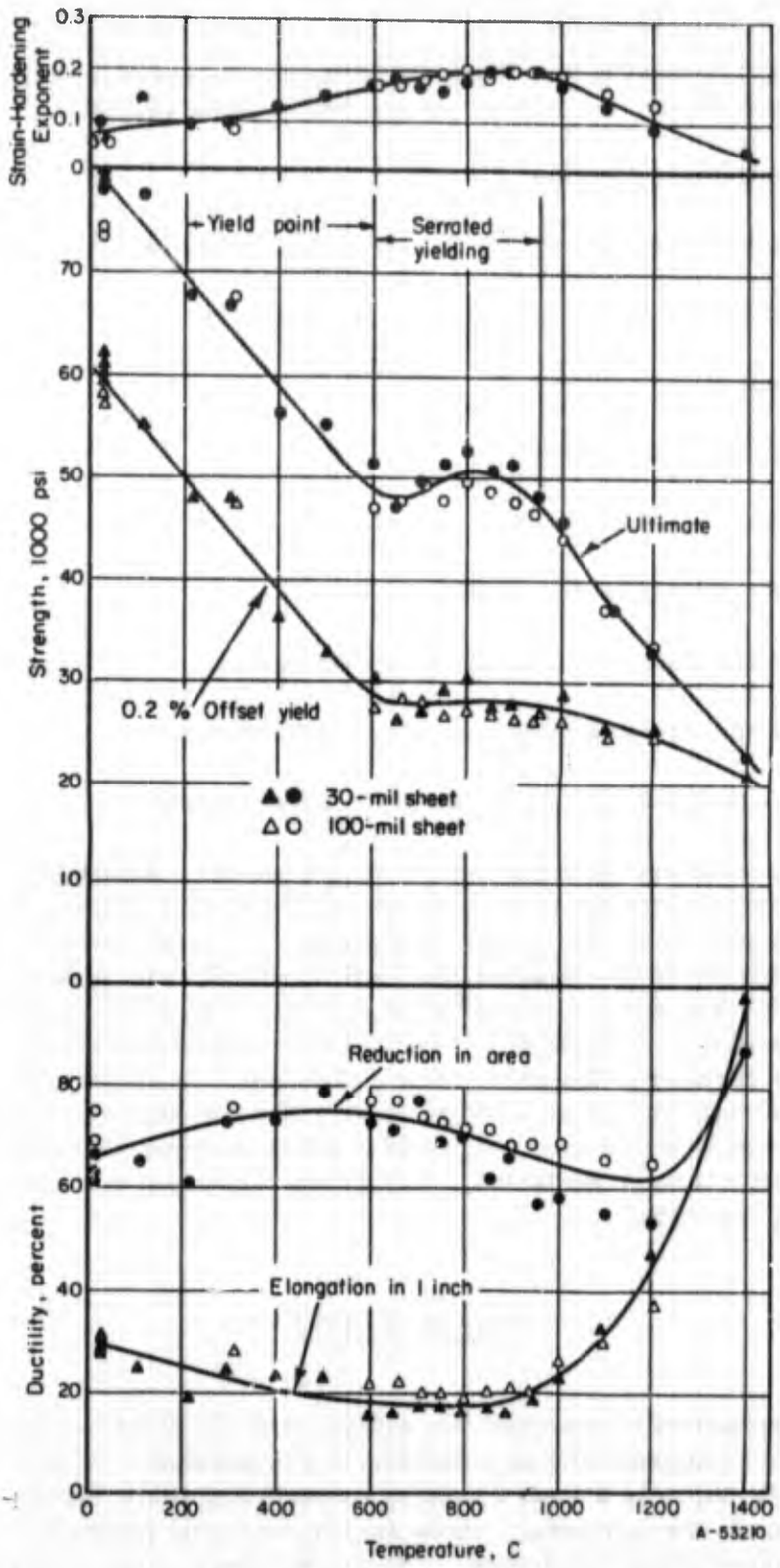

FIGURE 7. TENSILE PROPERTIES OF UNCOATED 30- AND 100-MIL Cb-752 SHEET IN VACUUM AT A STRAIN RATE OF 0.1 PER MINUTE

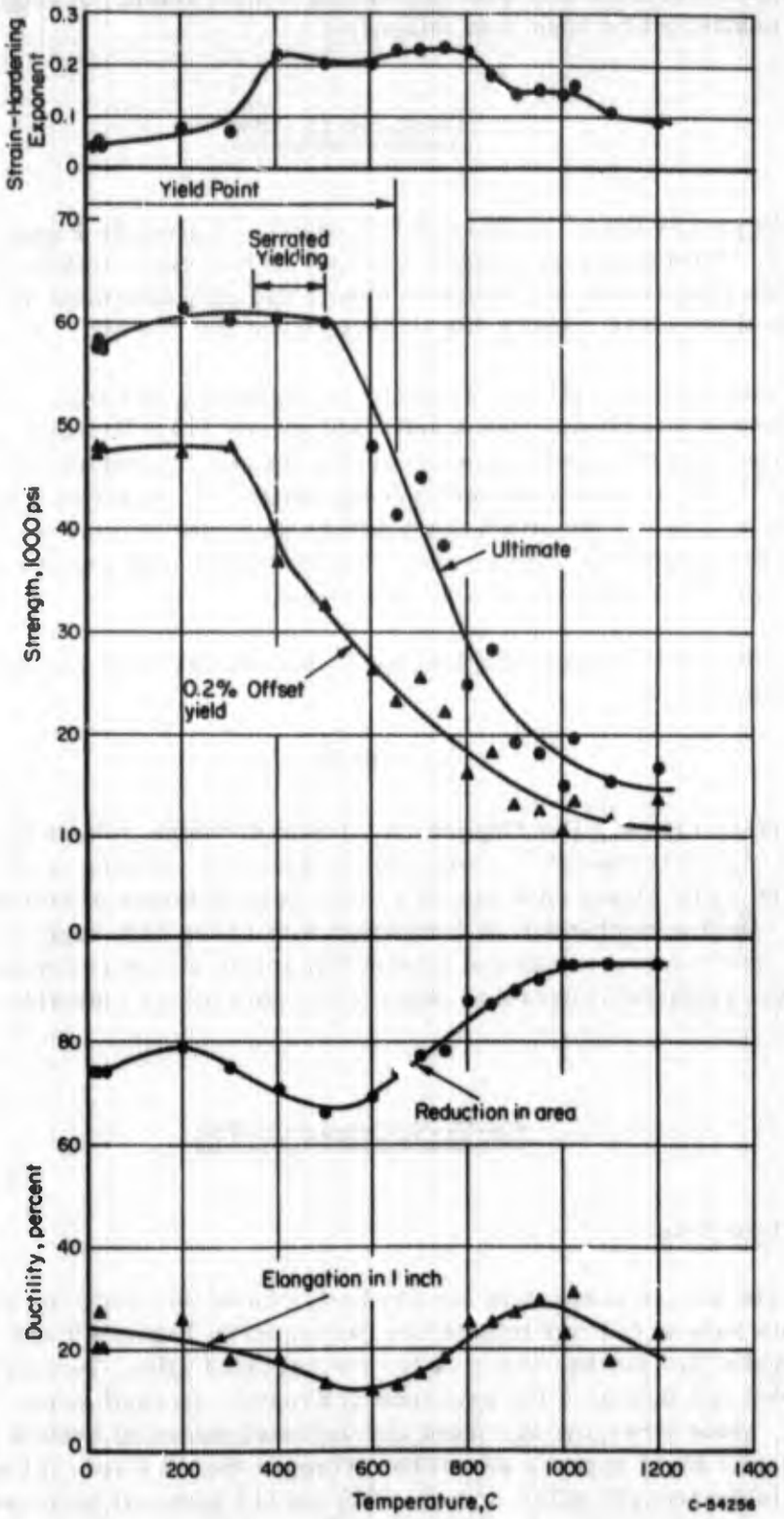

FIGURE 8. TENSILE PROPERTIES OF UNCOATED 30-MIL Cb-10W SHEET IN VACUUM AT A STRAIN RATE OF 0.1 PER MINUTE

Above 1000 C dynamic strengthening is no longer apparent. Strength decreases and elongation increases normally with increasing temperature. Strength and ductility are essentially unaffected by specimen thickness.

Uncoated Cb-10W

Tensile properties of 30-mil Cb-10W sheet are given in Figure 8 and Table 9 (Appendix C). Strengths stay roughly constant or increase slightly up to 500 C and then drop at higher temperatures. There is a mild ductility minimum around 500 C, but on the whole ductilities are comparable to those found for Cb-752.

In refractory metal alloys, dynamic strengthening is broadly associated with interaction between interstitial atoms and dislocations.[16, 17] Some experimental evidence indicates that the mechanism in columbium and columbium alloys is dynamic strain aging[13-15] or strain-induced precipitation.[13] In strain aging, the interstitial element responsible for the effect must diffuse at a rate similar to that of moving dislocations as determined by strain rate. For strain-induced precipitation, a certain amount of interstitial diffusion is also necessary.

A relation[18, 19] describing the occurrence of serrated yielding and strength peaks in columbium is

$$\dot{\epsilon} = 10^9 D, \qquad (2)$$

where $\dot{\epsilon}$ = strain rate and D = required minimum diffusion rate of the appropriate interstitial. The higher temperature required for serrated yielding in Cb-752 compared to Cb-10W at the same strain rate can be rationalized in terms of soluble zirconium decreasing D. Such a mechanism is consistent with creep data suggesting short-range interactions between zirconium and interstitial solute atoms at dislocation sites.[20] Moreover, the yield-point behavior observed in both alloys indicates additional interstitial effects.

Cr-Ti-Si Coated Cb-752

Air, Low Strain Rate

Substrate tensile properties for Cr-Ti-Si coated 30- and 100-mil Cb-752 sheet in air at a strain rate of 0.1 per minute are presented in Figures 9 and 10 and Tables 10 and 11 (Appendix C). As was the case for the uncoated alloy, serrated yielding was again observed and indicated the presence of dynamic strengthening. With increasing temperature, yield strengths of coated and uncoated material behave similarly. However, the 30-mil sheet appears somewhat stronger than the 100-mil sheet. Above 500 C, the yield-strength difference of ~5000 psi (15 percent) becomes significant compared to a scatter of ~2000 psi in the data. Ultimate strengths of the coated 30-mil sheet were also higher. Because of low fracture strengths and ductility, no peak in the ultimate strength was obtained in the dynamic strengthening temperature range 600-950 C.

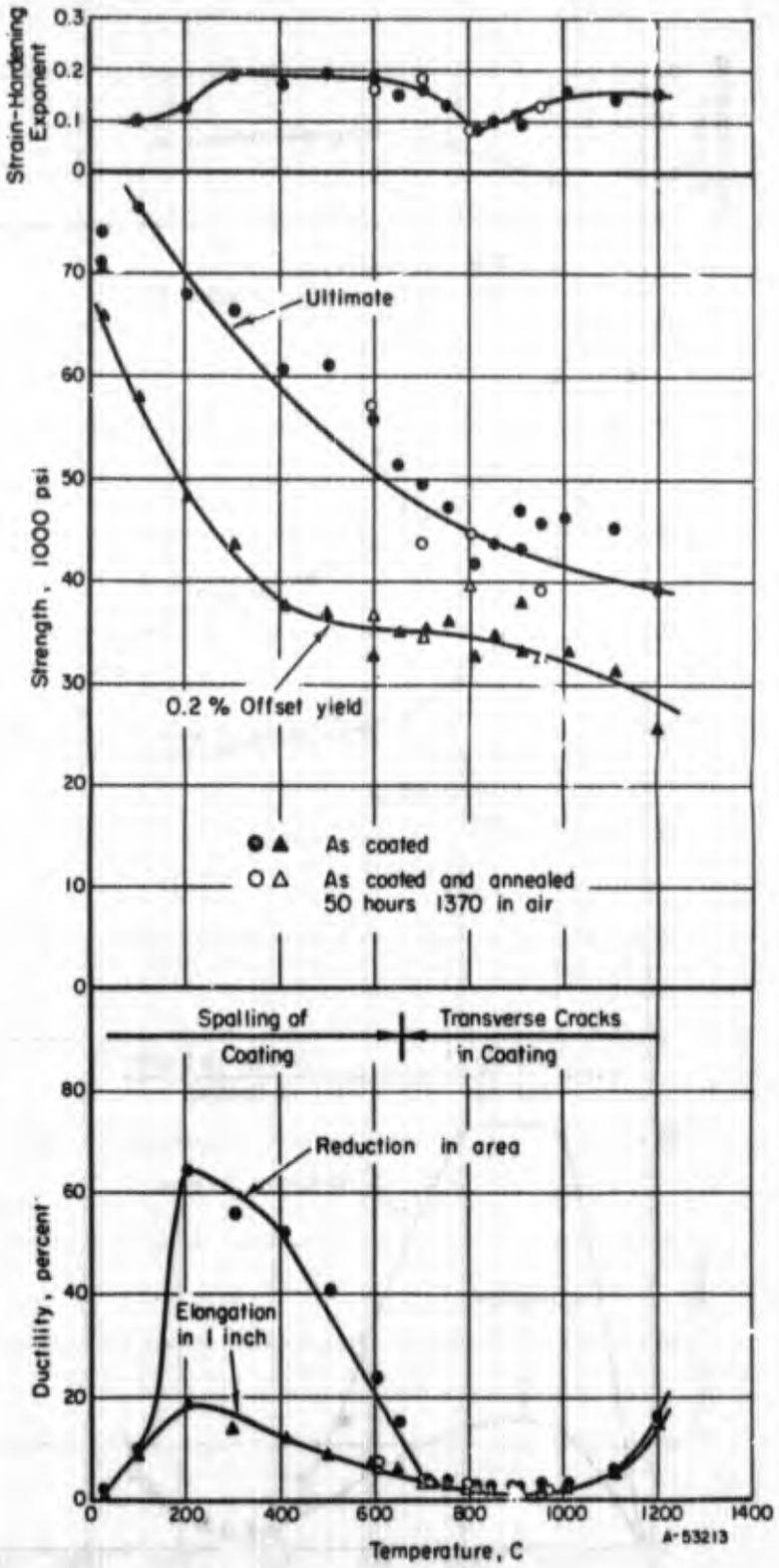

FIGURE 9. SUBSTRATE TENSILE PROPERTIES OF Cr-Ti-Si COATED 30-MIL Cb-752 SHEET IN AIR AT A STRAIN RATE OF 0.1 PER MINUTE

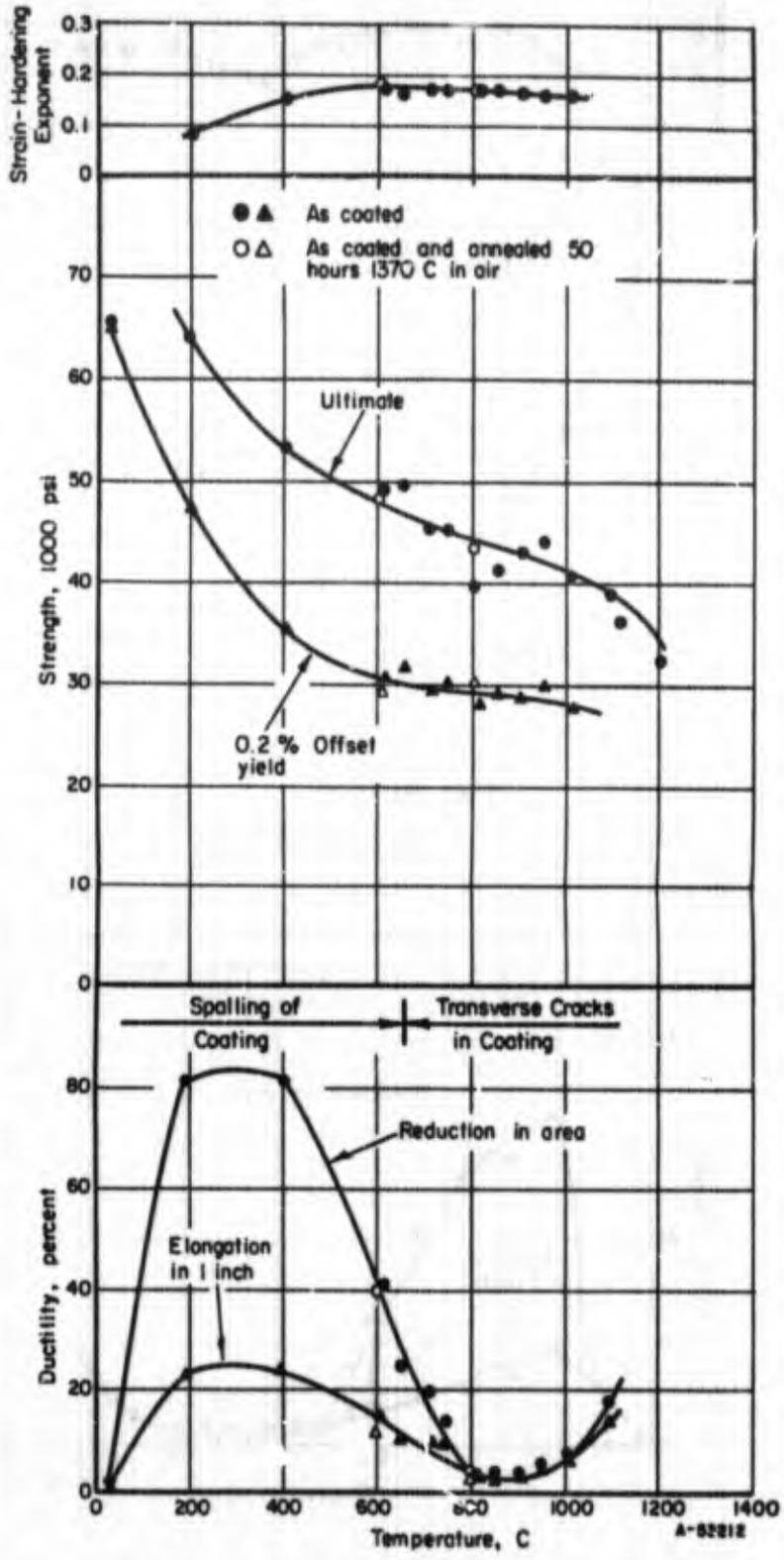

FIGURE 10. SUBSTRATE TENSILE PROPERTIES OF Cr-Ti-Si COATED 100-MIL Cb-752 SHEET IN AIR AT A STRAIN RATE OF 0.1 PER MINUTE

Elongations and reductions in area of both sheet thicknesses were drastically reduced relative to those of uncoated Cb-752 in vacuum. Ductility results are compared in Figure 11. The low ductility of coated Cb-752 at room temperature is believed to be the result of an increased ductility transition temperature caused by the coating. Up to ~600 C, reasonably high ductilities persisted and were accompanied by spalling of the coating and a shear-type fracture inclined to the tensile axis. A ductility minimum occurs in the temperature range ~700-1100 C. The thicker sheet was less severely embrittled (3-18 percent RA) than the thinner sheet (1-5 percent RA). An air anneal of 50 hours at 1370 C to thicken the subsilicide zone had little beneficial effect on ductility. A typical fracture is compared to that of uncoated Cb-752 tested in vacuum in Figure 12. There is an absence of necking, little spalling of coating near the fracture, profuse transverse coating cracks, and an irregular transverse fracture tending to follow coating cracks. The reason for the low ductility is apparent from Figure 13. Wedges containing debris (metallographically identified as a columbium oxide) formed at the base of coating cracks and permitted the surrounding atmosphere ready access to the substrate. It is likely that oxygen diffusion into the substrate caused progressive embrittlement and permitted coating cracks to propagate. As straining proceeded, the cracks rapidly enlarged until there was no load-bearing substrate left. Fracture accompanied by oxidation and contamination took place in only ~20 seconds, the usual test duration in the ductility minimum temperature range. Heat-up times were not considered because the specimen surface was static and adequately protected from oxidation by the coating.[7] Also of interest in Figure 13b is the smaller amount of oxidation of the Ti-Cr-enriched substrate immediately beneath the coating-substrate interface. However, neither the ductility nor the contamination resistance of this thin zone was sufficient to preclude cracking.

Above 900 C, ductility gradually rose and indicated increased dynamic protection by the coating during the test. Possible mechanisms include increased coating ductility and formation of a viscous protective glass.

Air, High Strain Rate

Figure 14 and Table 12 (Appendix C) summarize the tensile results for Cr-Ti-Si coated and uncoated Cb-752 sheet in air at a nominal strain rate of 100 per minute. Comparing the limited strength data with Figure 7, there appears to be reduction in ultimate strength at ~900 C as a result of increased strain rate. A negative strain rate sensitivity agrees with results presented in Phase 2. Furthermore strain hardening seems to peak around 1000 C compared with 850 C for specimens tested at 0.1 per minute. Such behavior suggests the dynamic strengthening region is pushed to higher temperatures by increasing strain rate and is consistent with Equation (2).

The ductility of coated 100-mil sheet remains high up to ~1000 C. Some loss in ductility is indicated for the 30-mil sheet at 950 C, but this is much less severe than similar material tested at the low strain rate. Spalling of the coating was noted in all tests. As shown in Figure 15, surface cracking to depths of 3-5 mils was noted adjacent to the fracture. These fissures did not propagate through the substrate, and ductile fractures similar to that in uncoated Cb-752 were obtained. Since the test duration was only ~0.1 second, oxygen apparently did not have sufficient time for inward diffusion and embrittlement of the substrate at the base of coating cracks. According to Figure 16,

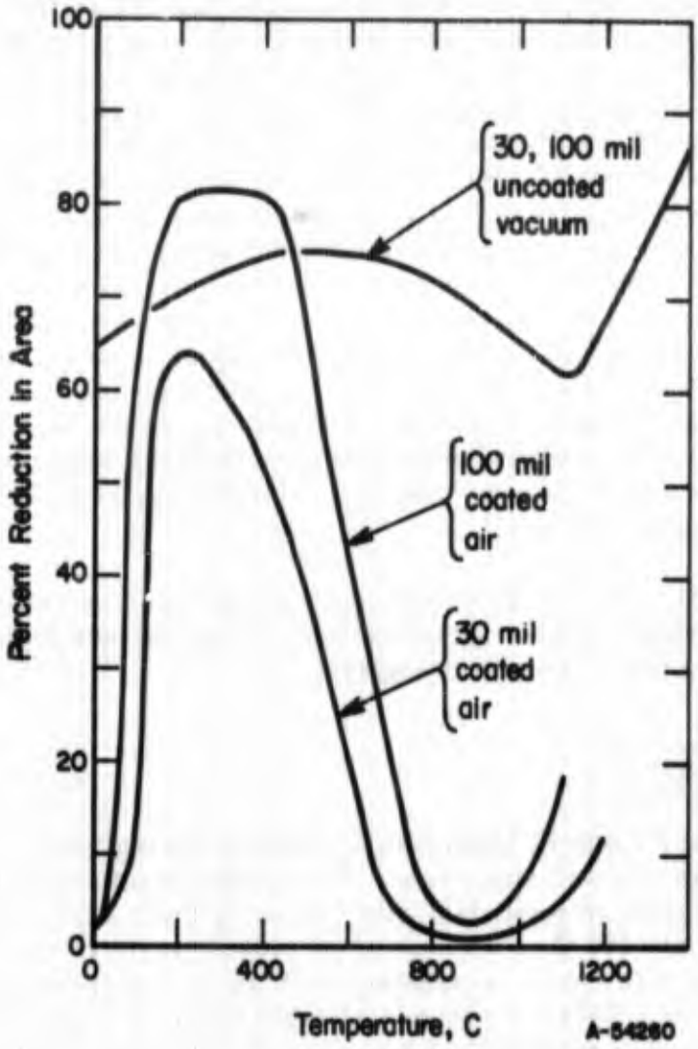

FIGURE 11. TENSILE DUCTILITY OF Cr-Ti-Si COATED 30- AND 100-MIL Cb-752 SHEET IN AIR COMPARED WITH THAT OF THE UNCOATED ALLOY IN VACUUM AT A STRAIN RATE OF 0.1 PER MINUTE

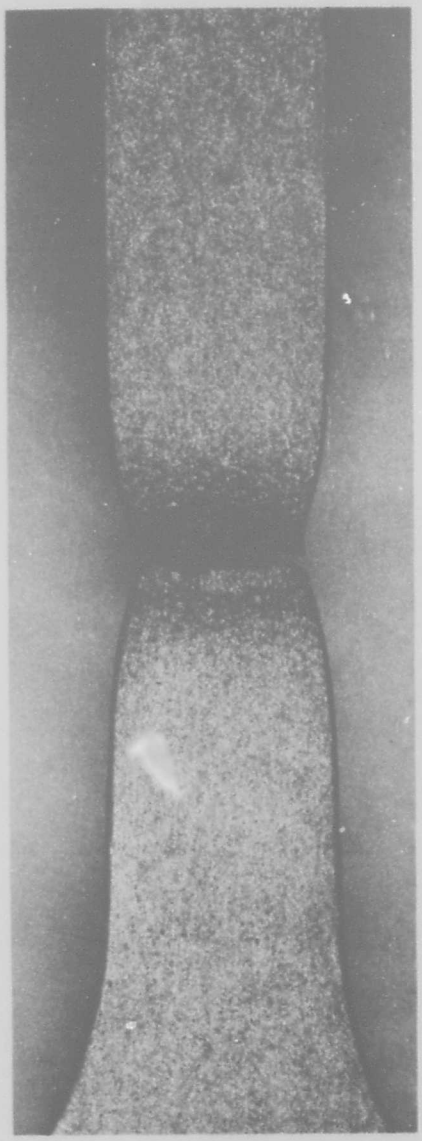

6X a. Uncoated, Vacuum IA720

20% elongation, 72% reduction in area.

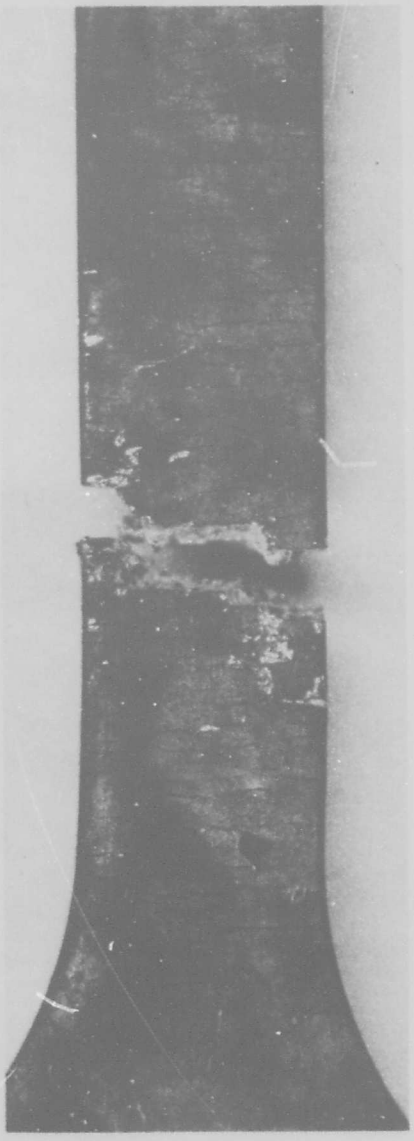

6X b. Cr-Ti-Si Coated, Air IA721

2.9% elongation, ~ 2.9% reduction in area.

FIGURE 12. FRACTURES OF UNCOATED AND COATED 100-MIL Cb-752 SHEET TESTED AT 850 C AT A STRAIN RATE OF 0.1 PER MINUTE

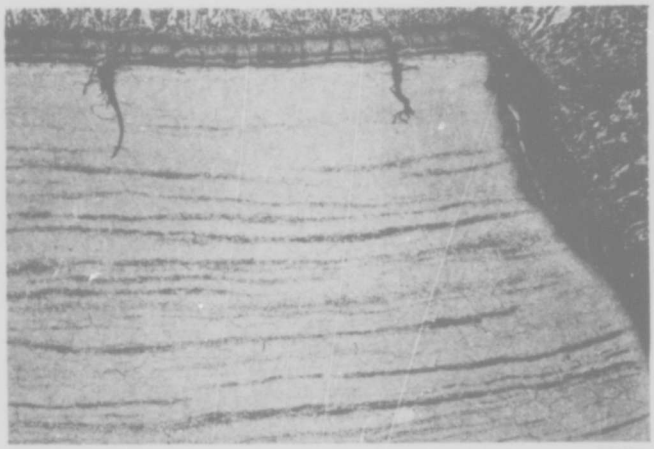

75X a. Fracture Area IA661

300X b. Near Fracture IA665

FIGURE 13. LONGITUDINAL MICROSTRUCTURES OF Cr-Ti-Si COATED 100-MIL Cb-752 SHEET TESTED AT 900 C IN AIR AT A STRAIN RATE OF 0.1 PER MINUTE

50 lactic acid – 30 HNO_3-2 HF etchant.

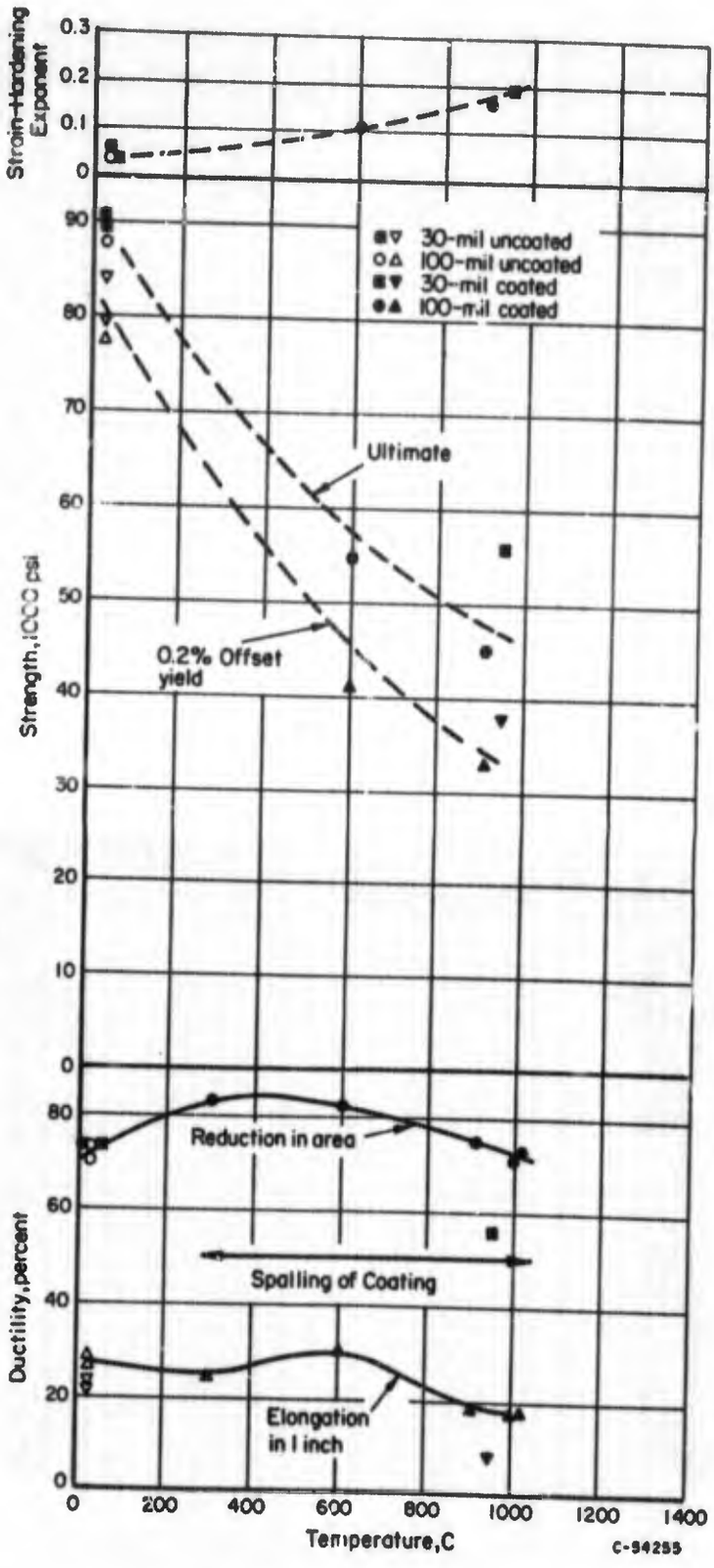

FIGURE 14. SUBSTRATE TENSILE PROPERTIES OF Cr-Ti-Si COATED Cb-752 SHEET IN AIR AT A STRAIN RATE OF 100 PER MINUTE

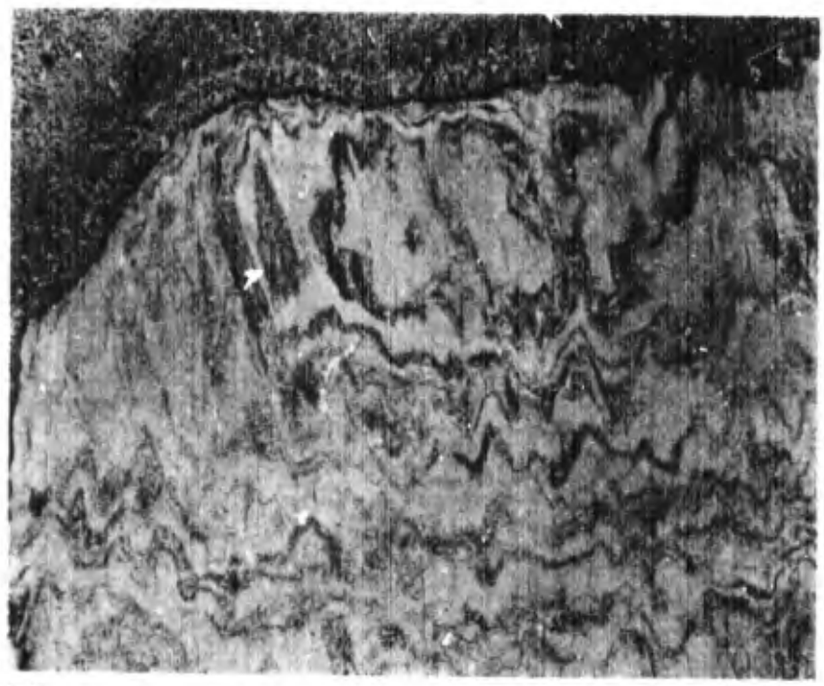

75X IA659

a. Uncoated, vacuum, 0.1 per minute strain rate

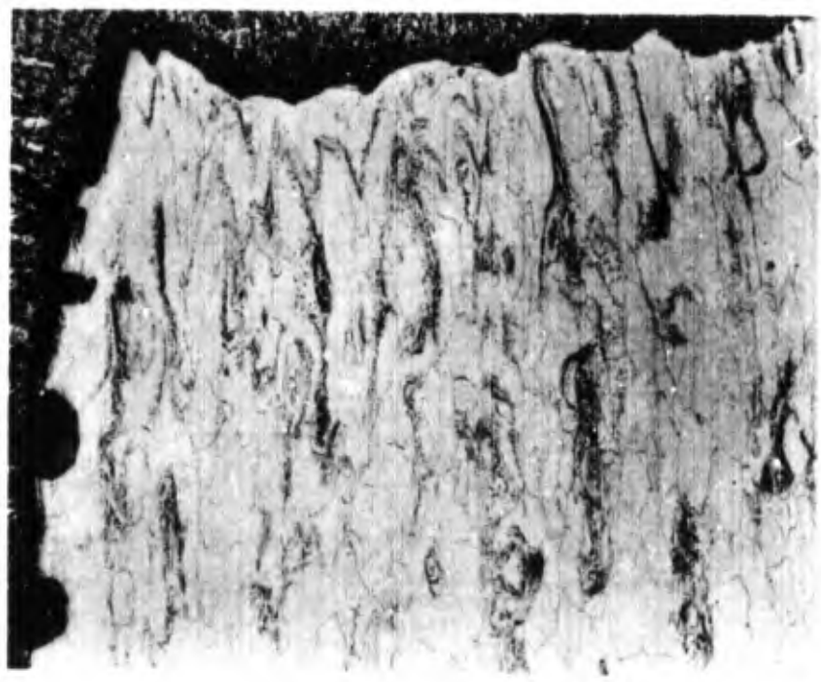

75X IA662

b. Cr-Ti-Si coated, air, 100 per minute strain rate

FIGURE 15. LONGITUDINAL MICROSTRUCTURES OF 100-MIL Cb-752 SHEET TESTED AT 900 C

50 lactic acid – 30 HNO_3 – 2 HF etchant.

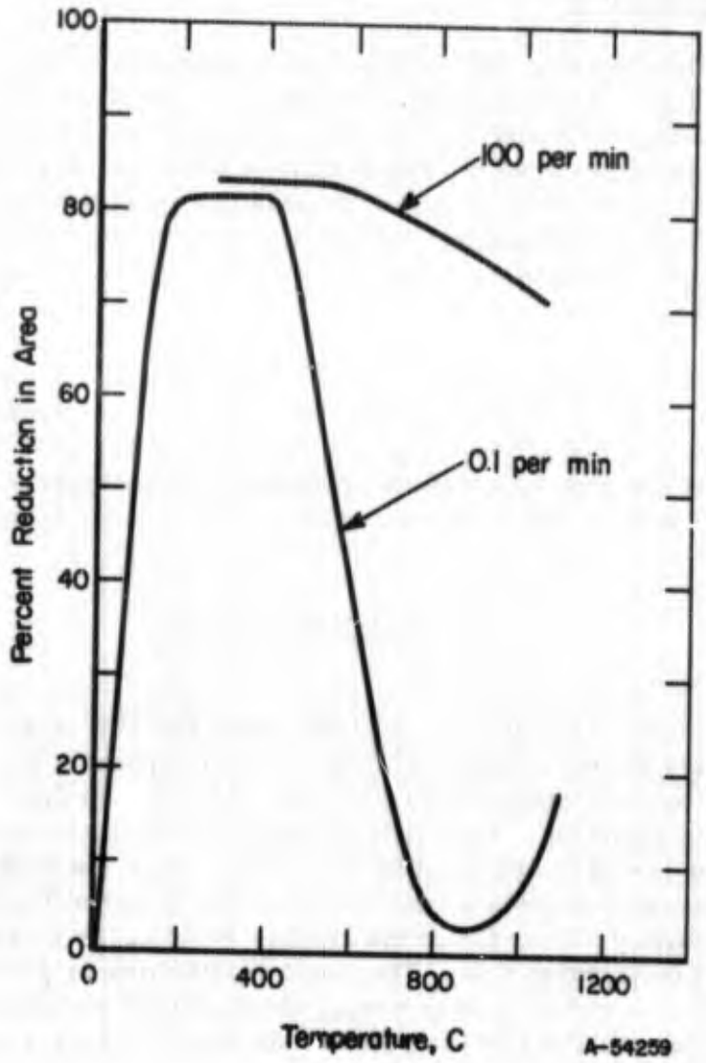

FIGURE 16. TENSILE DUCTILITY OF Cr-Ti-Si COATED 100-MIL Cb-752 SHEET IN AIR AT TWO STRAIN RATES

increasing strain rate 3 orders of magnitude apparently was beneficial to the ductility of coated Cb-752 in air. However, since the reduction in area remained ~70 percent at 25 C for both strain rates on uncoated material, strain rate per se is probably not an important factor in causing large ductility changes. Rather, a 200-fold reduction in exposure time during which contamination can occur most likely accounts for the high ductilities obtained for coated Cb-752 at the high strain rate.

Vacuum, Low Strain Rate

Substrate tensile properties of Cr-Ti-Si coated Cb-752 in vacuum tested at a strain rate of 0.1 per minute are given in Figure 17 and Table 13 (Appendix C). In comparison with Figures 9 and 10, the yield strengths are similar to those found in air. With the increased ductility, higher tensile strengths are realized and form the dynamic strengthening maximum in the temperature range 600-950 C. Up to 1000 C, fracture strengths are significantly higher than ultimate strengths. However, in the 1000-1300 C range, fracture and ultimate strengths are nearly equal, indicating little necking took place.

Up to 900 C ductilities remained high. Spalling of the coating and shear fractures were noted. Above 900 C, fractures were transverse, the coating adherent, transverse cracks prevalent, and ductilities lower. In the case of the lowest ductility found, Figure 18 shows that many coating cracks propagated a maximum of ~5 mils into the substrate and then blunted. The fracture tended to follow grain boundaries.

Cr-Ti-Si Coated Cb-10W

Substrate tensile results for Cr-Ti-Si coated Cb-10W in air at a strain rate of 0.1 per minute are given in Figure 19 and Table 14 (Appendix C). Up to 900 C strengths were lower than those of uncoated Cb-10W tested in vacuum (see Figure 8). No dynamic strengthening was apparent. The whole substrate cross section was affected since two coated specimens tested at 500 and 800 C in vacuum with the coating removed also exhibited lower strength and greater ductility than the material before coating. Based on other reported work[5], Ti or Cr on the surface could cause a chemical potential gradient and act as an interstitial sink. Therefore purification or gettering of some interstitials throughout the cross section during the Cr-Ti-Si coating process is a possibility. This effect was not noted in Cb-752 probably because the Zr formed stable interstitial compounds.

Above 600 C, the ductility was under 10 percent with a minimum of 2 percent occurring at ~900 C. As indicated in Figure 20, Cb-10W behaved similarly to Cb-752 in both coated and uncoated conditions. The major difference was that coated Cb-10W had significant room-temperature ductility, indicating a lower ductile-to-brittle transition temperature.

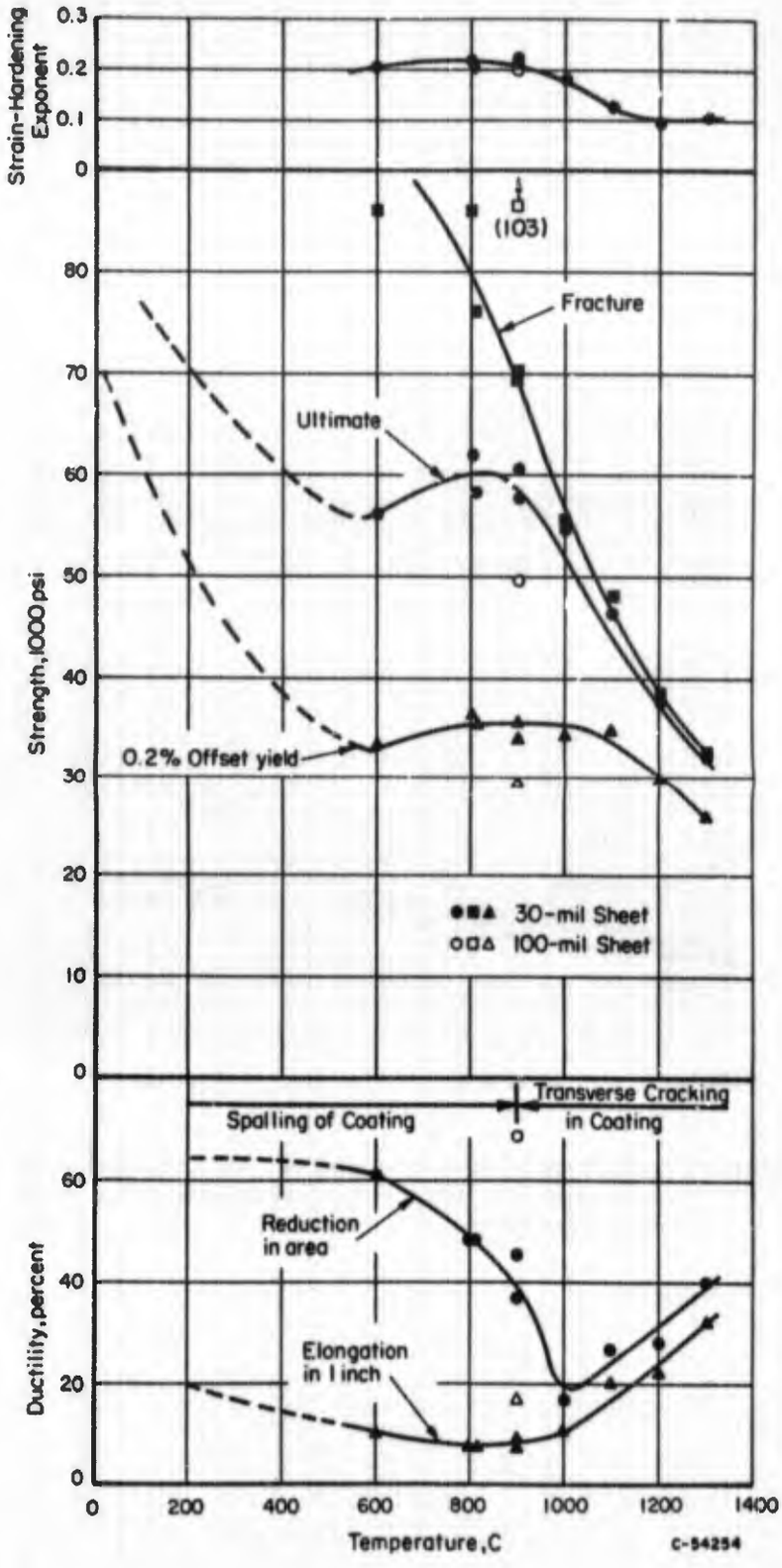

FIGURE 17. SUBSTRATE TENSILE PROPERTIES OF Cr-Ti-Si COATED Cb-752 SHEET IN VACUUM AT A STRAIN RATE OF 0.1 PER MINUTE

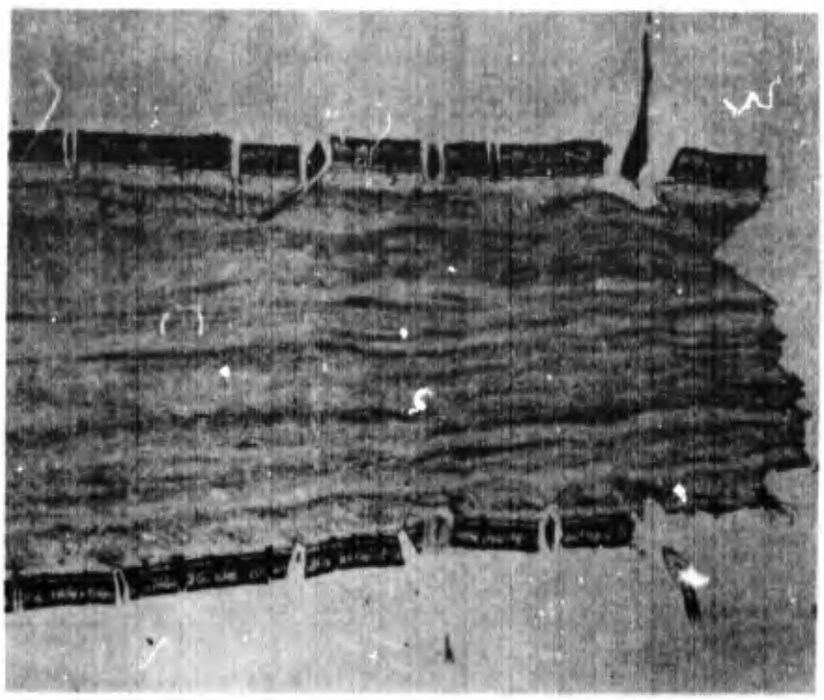

75X 50 lactic acid – 30 HNO_3 – 2 HF etchant. 8A837

FIGURE 18. LONGITUDINAL MICROSTRUCTURE OF Cr-Ti-Si COATED Cb-752 SHEET AT THE FRACTURE AFTER TENSILE TESTING IN VACUUM AT 1000 C AT A STRAIN RATE OF 0.1 PER MINUTE

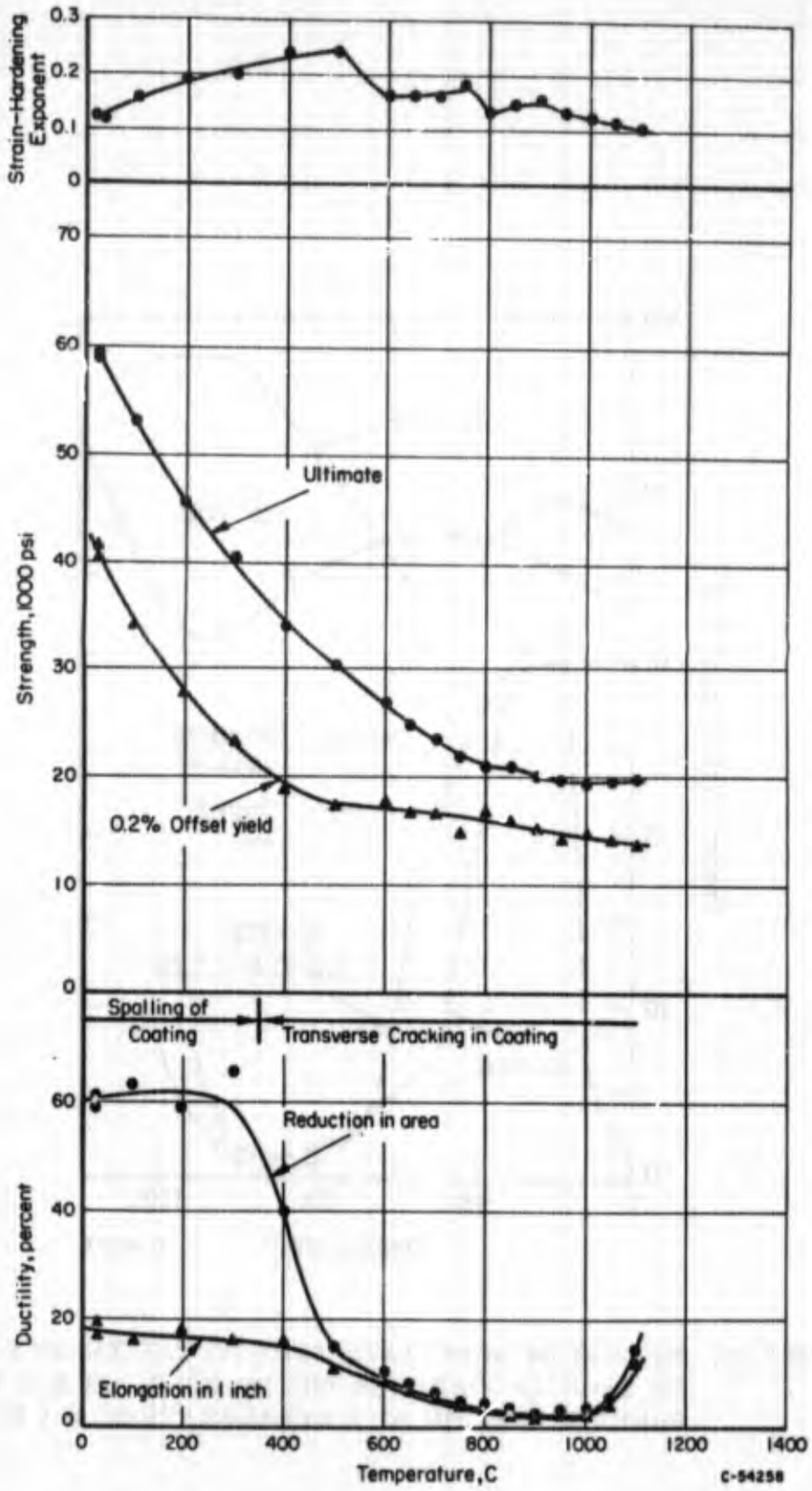

FIGURE 19. SUBSTRATE TENSILE PROPERTIES OF Cr-Ti-Si COATED 30-MIL Cb-10W SHEET IN AIR AT A STRAIN RATE OF 0.1 PER MINUTE

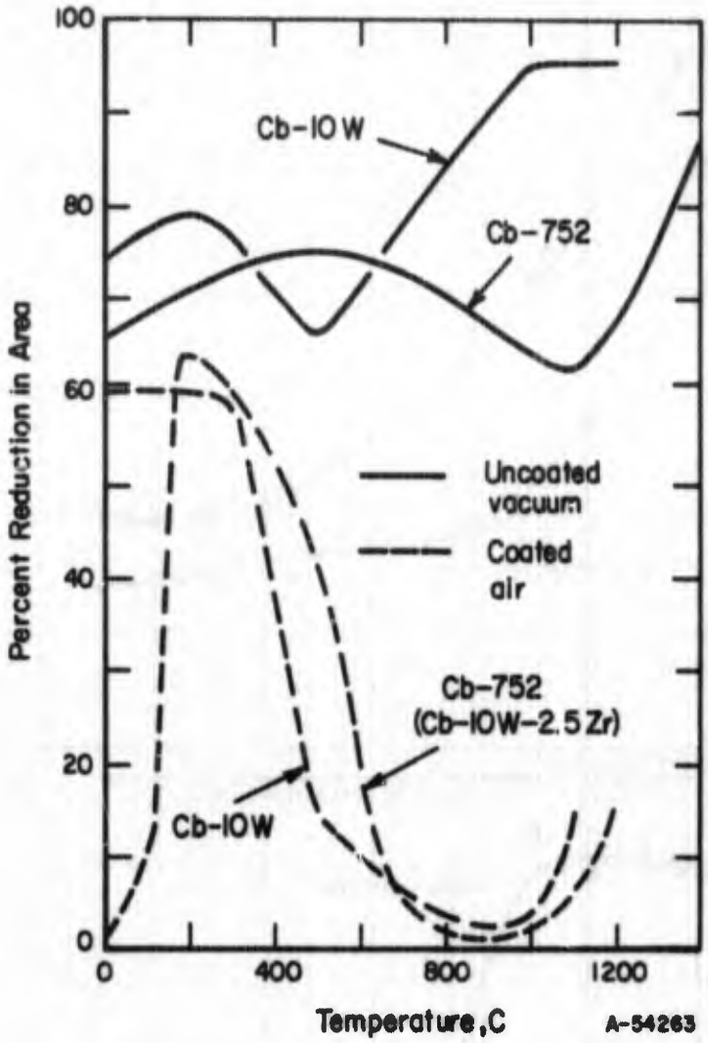

FIGURE 20. EFFECT OF SUBSTRATE TYPE ON THE TENSILE DUCTILITY OF Cr-Ti-Si COATED 30-MIL SHEET IN AIR AND UNCOATED SHEET IN VACUUM AT A STRAIN RATE OF 0.1 PER MINUTE

Ag-Si-Al-Mo Coated Cb-752

Substrate tensile properties found for Ag-Si-Al-Mo coated Cb-752 in air at a strain rate of 0.1 per minute are given in Figure 21 and Table 15 (Appendix C). Again yield strengths approximated those found from similar tests on Cr-Ti-Si coated 30-mil Cb-752 (see Figure 9). The slightly higher strengths (~3000 psi) noted up to ~400 C may have been caused by the ductile silver-rich layer bearing some measurable load. At 800-900 C the ultimate strength showed a maximum. Since strain-hardening exponents peak around 900 C, and since serrated yielding was noted, dynamic strengthening was still present.

Ductilities of Cb-752 in air with Cr-Ti-Si and Ag-Si-Al-Mo coatings are compared in Figure 22. Up to 750 C the silver-base coating remained solid and gave similar ductility behavior. Above 750 C, the coating reservoir became liquid and resulted in some improvement. Figure 23 illustrates this behavior. At 700 C, the coating was solid and internal cracks formed in the brittle disilicide layer and propagated into the substrate. The silver was unable to exclude air since traces of oxide were visible at the crack tips. At 800 C the coating was liquid and offered some protection by filling the cracks in the brittle coating layer. However, reduction in area only rose from 2 to ~6 percent compared with ~70 percent for uncoated material. This recovery was small probably because of liquid metal embrittlement and/or oxygen diffusion through the liquid Ag-Al alloy. Furthermore, holding the coated specimen in situ 1-4 hours at 1100 C before testing had little effect on ductility.

Factors Affecting Ductility

Zirconium Content of Substrate

Since similar ductilities were found for Cr-Ti-Si coated Cb-10W and Cb-752 (Cb-10W-2.5Zr) tested in air (see Figure 20), zirconium in Cb-10W does not seem to be a major factor in the ductility minimum behavior in the critical temperature range 700-1100 C. Since prior work[3] indicated that coated zirconium-containing columbium alloys were more susceptible to embrittlement in bending than unalloyed columbium, the presence of tungsten may be a contributing factor.

Dynamic Strengthening of Substrate

Dynamic strengthening was found in Cb-10W at 400-500 C and in Cb-752 at 600-950 C. Because the application of coatings to both materials resulted in a severe ductility minimum at temperatures from ~700 to 1100 C, the occurrence of dynamic strengthening in Cb-752 at these temperatures is probably coincidental.

Environment

The results show that the presence of air is detrimental to ductility and the major cause of the ductility minimum behavior found in coated Cb-10W and Cb-752.

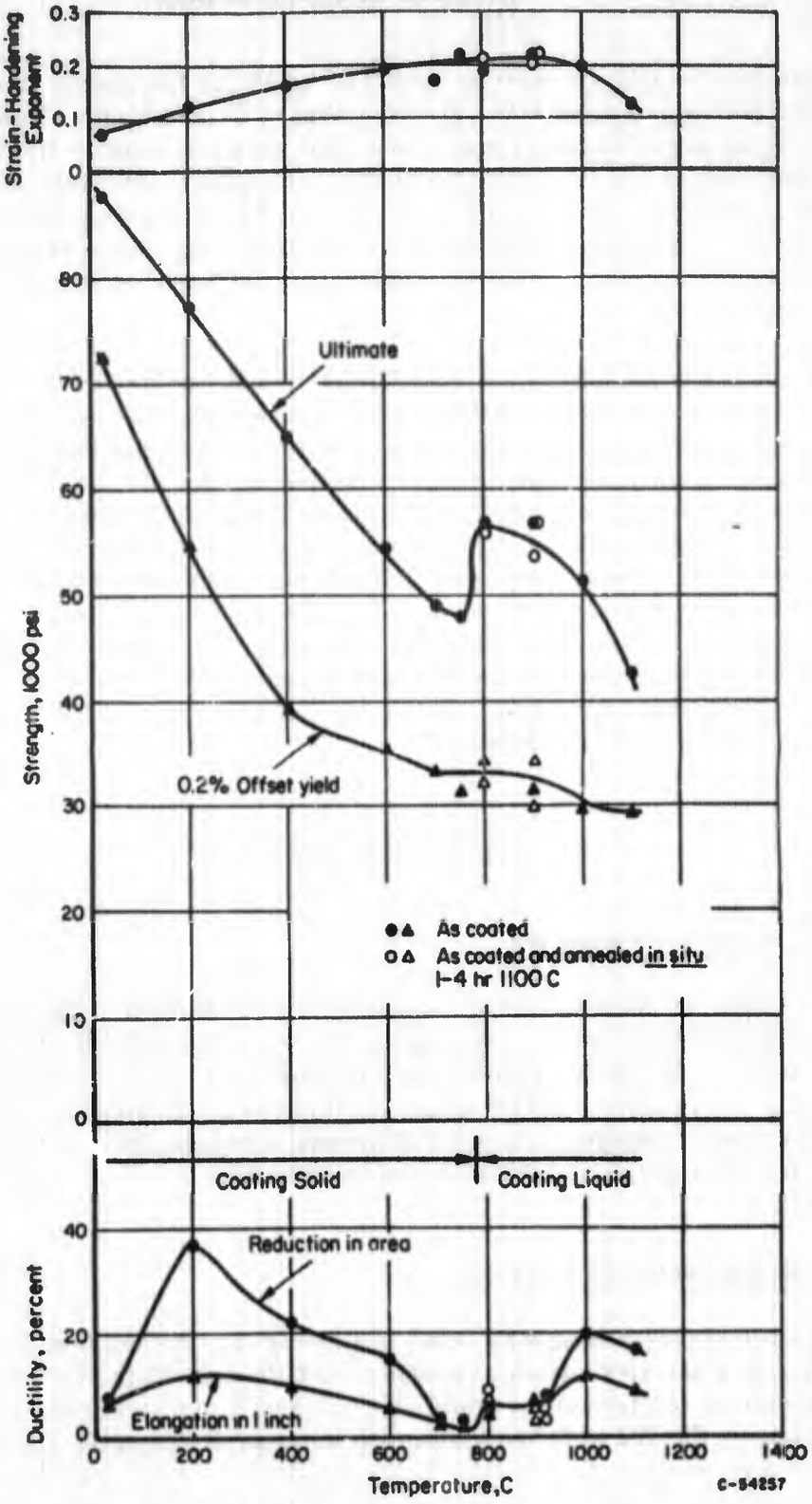

FIGURE 21. SUBSTRATE TENSILE PROPERTIES OF Ag-Si-Al-Mo COATED 30-MIL Cb-752 SHEET IN AIR AT A STRAIN RATE OF 0.1 PER MINUTE

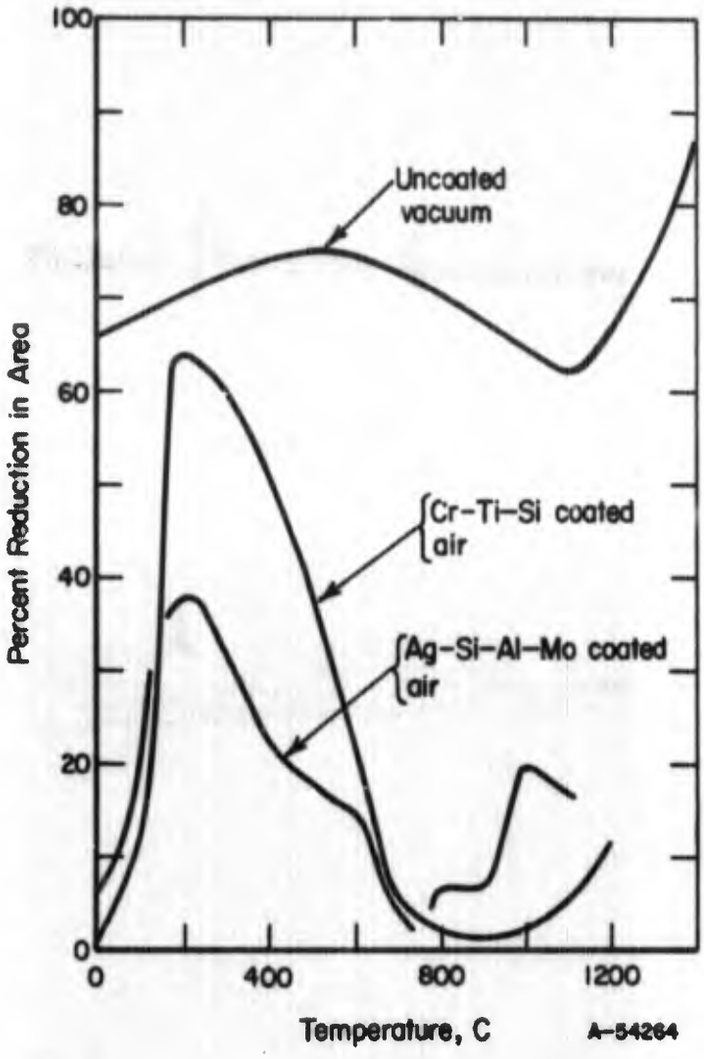

FIGURE 22. EFFECT OF COATING TYPE ON THE TENSILE DUCTILITY OF 30-MIL Cb-752 SHEET IN AIR AT A STRAIN RATE OF 0.1 PER MINUTE

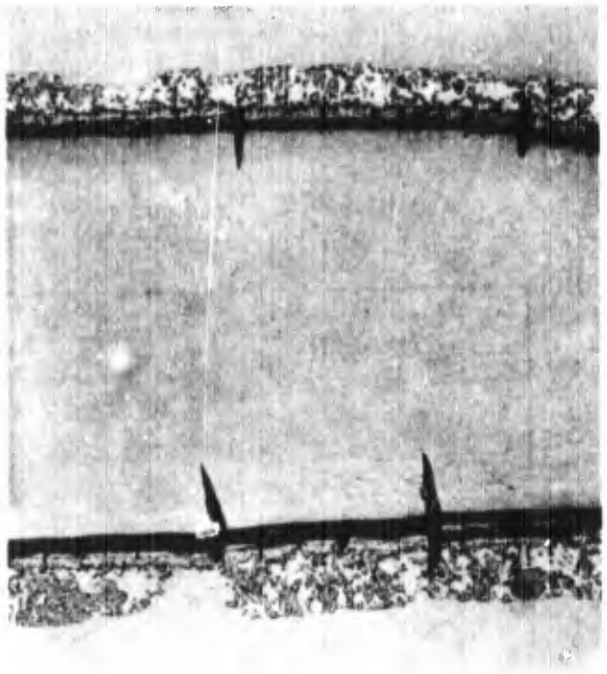

75X a. 700 C (Coating Solid) 5A753

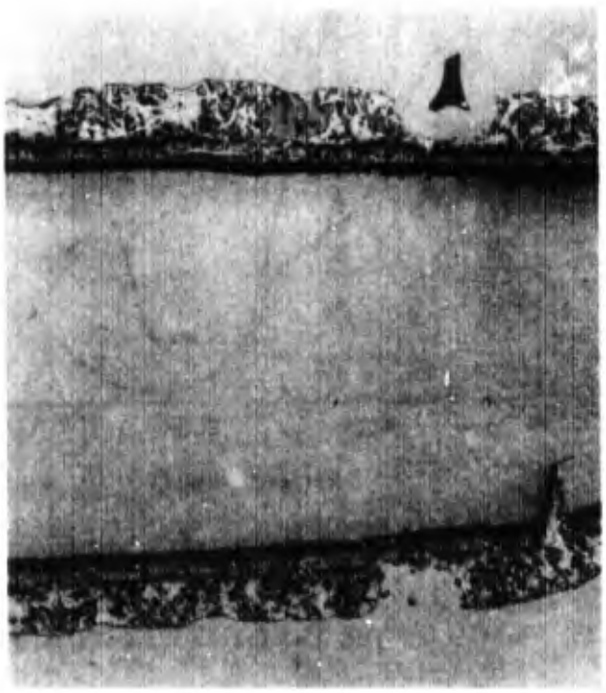

75X b. 800 C (Coating Liquid) 5A754

FIGURE 23. LONGITUDINAL MICROSTRUCTURES OF Ag-Si-Al-Mo COATED 30-MIL Cb-752 SHEET NEAR THE FRACTURE AFTER TENSILE TESTING IN AIR AT A STRAIN RATE OF 0.1 PER MINUTE

50 lactic acid – 10 HNO_3 – 2 HF etchant.

The extent of the effect, illustrated in Figures 12 and 13, is clearly shown in Figure 24 by comparing results for Cr-Ti-Si coated 30-mil Cb-752 sheet tested in air and vacuum. In the ductility minimum range 700-1100 C, the reductions in area rise from 1-5 percent to 20-55 percent by excluding air. Moreover, the lower limit of the ductility minimum range corresponds to the start of rapid oxidation in columbium.[21] In spite of a possible reduction in oxygen diffusion rate caused by the presence of zirconium as suggested by Equation (2), the mechanism was apparently ineffective in reducing embrittlement of Cb-752 at a strain rate of 0.1 per minute.

Mechanical Interaction Between Coating and Substrate

In Figure 24, the ductility of Cr-Ti-Si coated 30-mil Cb-752 sheet tested in vacuum was 20-55 percent compared with 60-75 percent for the uncoated alloy. The probable reason for the difference is believed to be mechanical interaction between coating and substrate.

In an effort to evaluate mechanical interaction effects, the residual stress pattern of Cr-Ti-Si coated Cb-752 sheet was changed by air annealing for 50 hours at 1370 C. A subsilicide layer (Figure 2b) that had a low thermal expansion coefficient presumably was compressed on cooling to room temperature. Calculations, summarized in Table 3 (see Appendix A for derivation of equations and discussion of their limitations), indicate that the maximum longitudinal elastic stress in the coated condition should be appreciably different from that in the coated plus annealed condition. Furthermore, it was thought that cracks in the disilicide layer in tension might be arrested by the compressed subsilicide layer, thereby excluding oxygen from the substrate. Results given in Figures 9 and 10 indicate little ductility differences between the two stress conditions in both sheet thicknesses. Therefore, it is concluded that the subsilicide layer offered no additional dynamic protection from coating cracks or atmosphere.

TABLE 3. ESTIMATES OF MAXIMUM LONGITUDINAL ELASTIC STRESSES IN Cr-Ti-Si COATED Cb-752 SHEET AT 25 C AS A RESULT OF DIFFERENTIAL THERMAL EXPANSION ACCORDING TO APPENDIX A

	Maximum Longitudinal Stress, 1000 psi	
	30-Mil Sheet	100-Mil Sheet
	As Coated at 1120 C	
Disilicide layers	68-135 tension	87-173 tension
Substrate	19 compression	7 compression
	As Coated and Air Annealed 50 Hours at 1370 C	
Disilicide layer	35-62 tension	44-83 tension
Subsilicide layer	62-72 compression	83-88 compression
Substrate	2-6 tension	1-3 tension

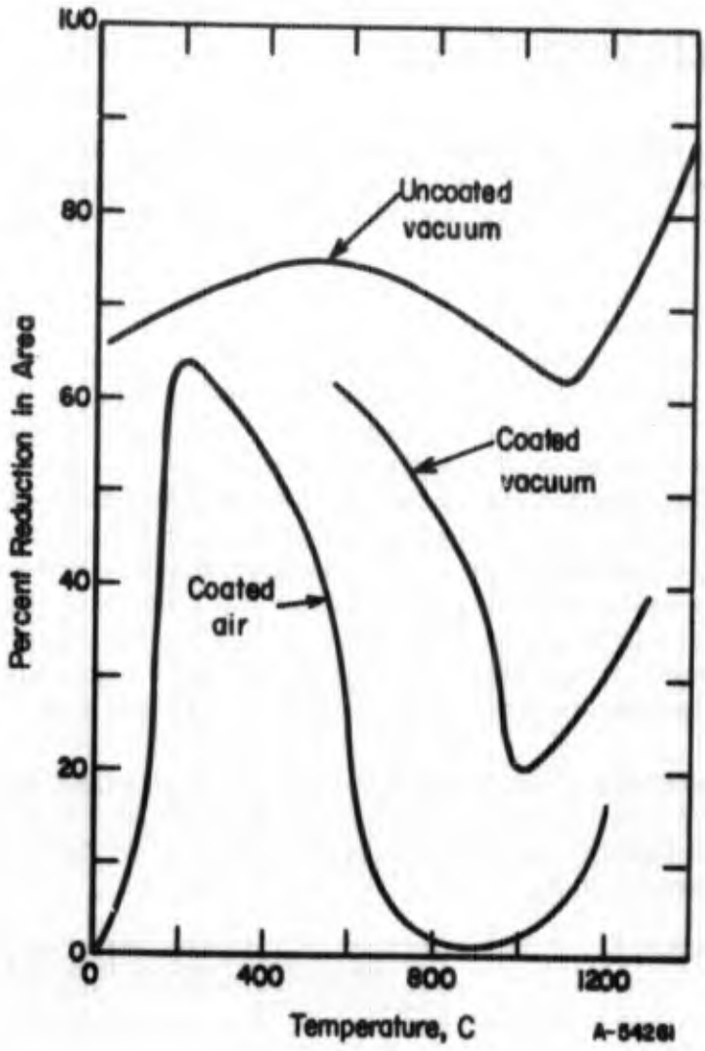

FIGURE 24. EFFECT OF ENVIRONMENT AND PRESENCE OF Cr-Ti-Si COATING ON THE TENSILE DUCTILITY OF 30-MIL Cb-752 SHEET AT A STRAIN RATE OF 0.1 PER MINUTE

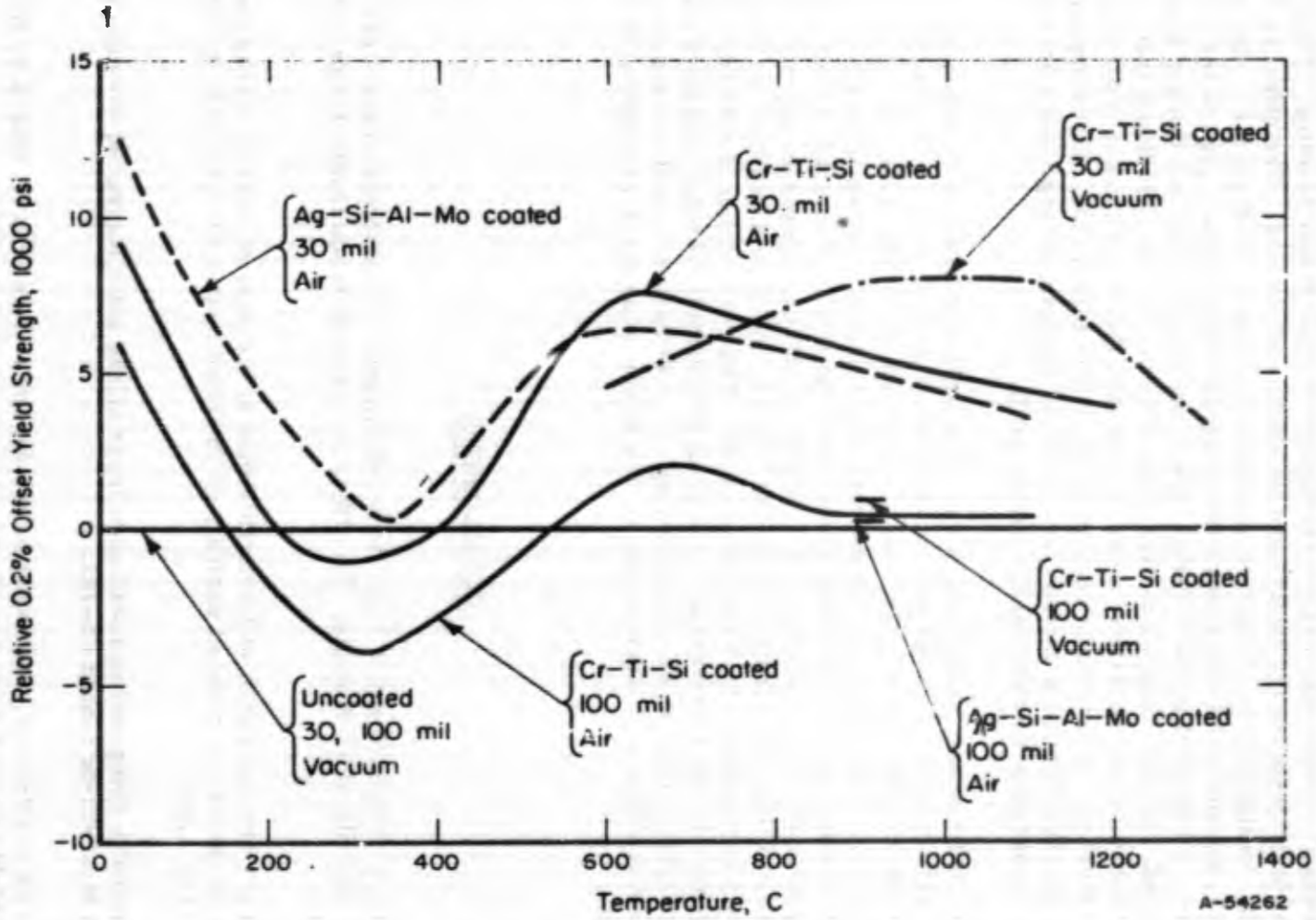

FIGURE 25. SUBSTRATE YIELD STRENGTH OF COATED 30- AND 100-MIL CB-752 SHEET RELATIVE TO THAT OF THE UNCOATED ALLOY IN VACUUM AT A STRAIN RATE OF 0.1 PER MINUTE

Cracks in the coating set up notches near the coating-substrate interface. Associated with these notches are triaxial stresses along with bond-shear and normal stresses. These localized stresses can be considered as mechanical interactions between coating and substrate. The notch effect is illustrated in Figures 15b and 18. Even though the Cb-752 substrate behaved in a ductile manner, coating cracks provided crack initiation sites and many cracks propagated ~5 mils before blunting. This action evidently led to grain-boundary failure and prevention of necking. The effect is further illustrated by similarities in elongation and reduction in area in Figure 17. Since the blunted cracks consumed ~33 percent of the load-bearing substrate area in the 30-mil sheet and only ~10 percent in the 100-mil sheet, one would expect the thicker sheet to be less affected. Indeed, this is the case since Figures 14 and 17 indicate that Cr-Ti-Si coated 100-mil Cb-752 sheet was more ductile than the thinner sheet in air at a strain rate of 100 per minute or in vacuum at the lower strain rate. Since apparent mechanical interaction effects extend above 1000 C, dynamic strengthening does not enter into consideration since it ceases above 950 C.

Further indication of coating-substrate mechanical interaction is given by comparison of yield strength of coated and uncoated Cb-752 sheet in air and vacuum in Figure 25. In spite of ±2000 psi scatter, the data indicate the substrate is stronger than the uncoated alloy. The effect of diffused elements from the coating is probably unimportant. The reason is that two coating conditions (as Cr-Ti-Si coated, or Ag-Si-Al-Mo coated) give about the same strengths. These conditions represent two different concentration profiles, the former containing Cr, Ti, and Si to a depth of ~0.5 mil, the latter probably containing Si to a negligible depth. The overcoming of residual compressive stresses in the substrate as a result of differential thermal expansion (Appendix A) might explain some of the strengthening. The remainder could be caused by the coating restricting flow of surface material, the effect being more pronounced in the thinner sheet.

CONCLUSIONS

(1) Zirconium content (0 and 2.5 percent) and dynamic strengthening have little effect on the ductility of TRW coated Cb-10W in the critical temperature range 700-1100 C.

(2) Air causes contamination and embrittlement at the base of coating cracks and is the major factor for reduced ductility of Cr-Ti-Si coated Cb-10W and Cb-752 (Cb-10W-2.5Zr).

(3) An apparently compressed subsilicide layer offers little increased dynamic protection to Cr-Ti-Si coated Cb-752.

(4) Compared to Cr-Ti-Si, somewhat better dynamic protection is offered by Sylcor Ag-Si-Al-Mo coating when the Ag-Al alloy is liquid above 750 C.

(5) Mechanical interaction between coating and substrate apparently has a measurable detrimental effect on the ductility of Cr-Ti-Si coated Cb-752. This effect increases with decreasing substrate thickness from 100 to 30 mils.

(6) Since the substrate 0.2 percent yield strength is maintained and the low ductility is measurable, the embrittlement may not be a limiting factor in the use of coated columbium alloy systems designed to operate below the yield strength.

PHASE 2. DYNAMIC STRENGTHENING DURING CREEP OF COLUMBIUM ALLOYS

INTRODUCTION

It was demonstrated in Phase 1 that the addition of Zr to a Cb-10W alloy raises the range of temperatures where dynamic strengthening is observed in tension tests: ~200-500 C for Cb-10W (Figure 8) and ~600-950 C for Cb-10W-2.5Zr (Figure 7). The results on Cb-10W are very similar to those reported for unalloyed Cb[14, 15]. In addition to the strength peaks, other associated phenomena are serrated yielding and negative strain-rate sensitivity. The presence of both effects was found in the Cb-10W-2.5Zr alloy, as shown in Figure 26. A general explanation of this behavior in terms of the dynamic behavior of dislocations has been given by Wilcox and Rosenfield[29].

Based on previous data in the literature it is reasonable to expect that a dynamic strengthening process should also be reflected in an improved elevated-temperature creep strength. For example, in 1954, Cottrell[30] suggested that during a creep test, the onset of strain aging should lead to the suppression of recovery, and hence a decrease in the creep rate. He based this conclusion on the results of Dumbleton[31], who found this to be the case for zinc single crystals containing nitrogen, and the work of Glen[32], who observed a similar effect in steel. More recently Borch, Shepard, and Dorn[33] noted that the activation energy for creep of Al-3.2 at .% Mg was anomalously high over the temperature range of ~RT to 120 C. The activation-energy peak occurred over approximately the same temperature range where serrated yielding was observed in normal tension tests. Borch, et al., ascribed the high activation energies to Cottrell locking, the activation energy being the sum of that for cross-slip and unlocking of dislocations. Gregory and Rowe[20] conducted similar creep studies on Cb-1Zr alloy. Although their data were not complete, they observed a tendency toward a peak in a plot of activation energy versus temperature at slightly less than ~1000 C. From Chang's[13] data it appears that this temperature is near the upper limit of the temperature range where serrated yielding is observed in tension tests.

Therefore, the purpose of this phase of the program was to examine the effects of dynamic strengthening on the creep behavior of Cb alloys. Emphasis was placed on studying the influence of Zr additions on the creep rate over the temperature range ~800-1200 C.

MATERIALS

The Cb-752 and Cb-10W alloys used in this phase were from the same heats as those in Phase 1. Creep specimens had configurations identical to tensile specimens (Figure 6) and they were machined from sheets that had been surface ground from 0.120 to 0.080-inch thickness. The final recrystallization anneal for both alloys was 1 hour at 1700 C, which resulted in a grain size of a ~0.1 mm for both alloys. The microstructures of the uncrept alloys were similar to those in Figure 1 except for a slightly

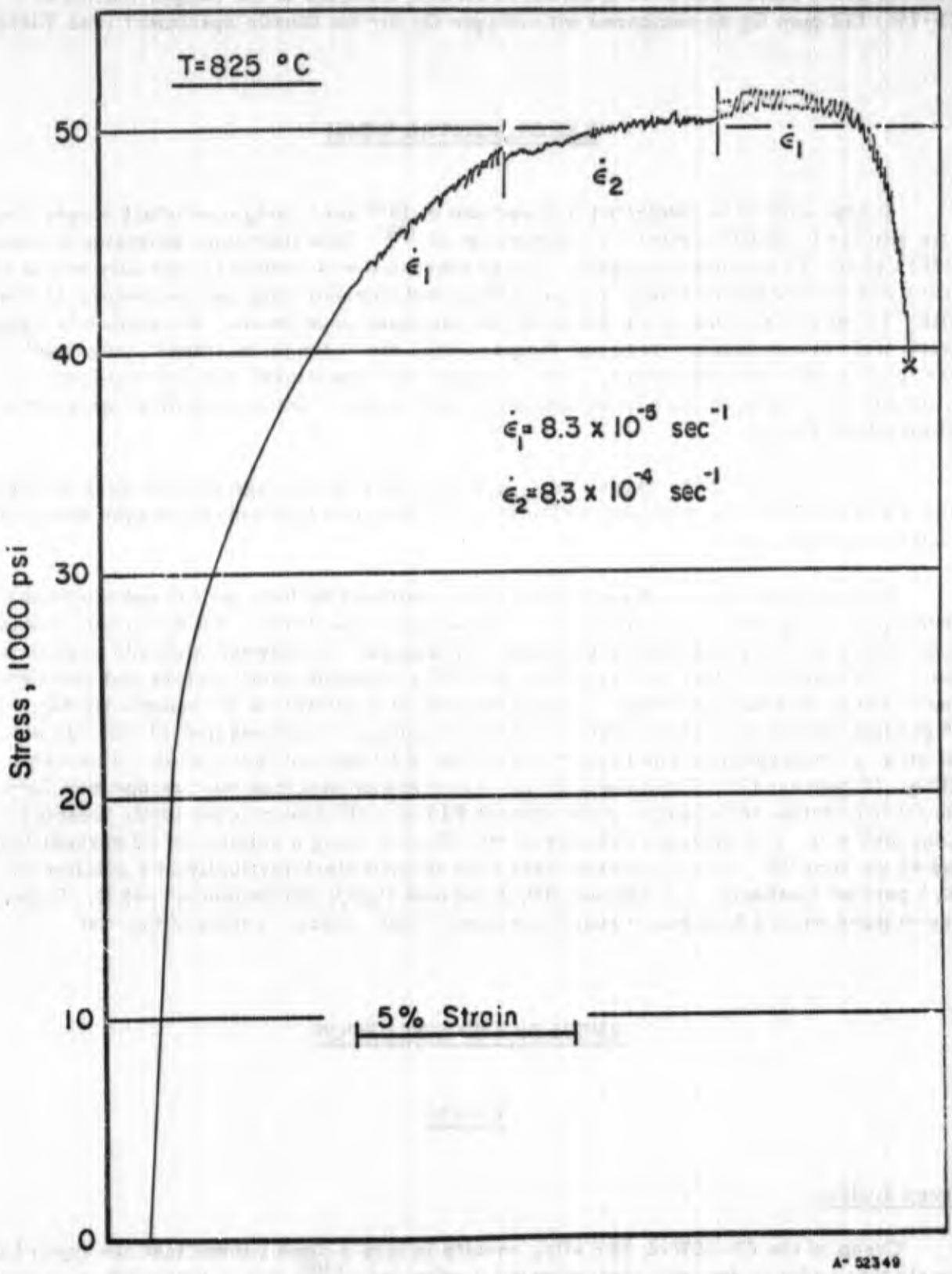

FIGURE 26. STRAIN-RATE-CYCLING TESTS ON A RECRYSTALLIZED Cb-752 SPECIMEN SHOWING SERRATED YIELDING AND NEGATIVE STRAIN-RATE SENSITIVITY

coarser grain size. The 1700 C anneal caused an increase in the oxygen content of Cb-752; 112 ppm O_2 as compared with 29 ppm O_2 for the tensile specimens (see Table 1).

EXPERIMENTAL WORK

Creep tests were conducted in a vacuum of 10^{-6} torr using a constant stress lever arm similar to that described by Fullman, et al.[34] This technique maintains a constant stress up to ~10 percent elongation. Creep extension was measured optically with a sensitivity of 50-100 microinches, by two sliding molybdenum strip extensometers scribed with fiducial marks, one on each side of the specimen gage length. In addition to normal creep tests at a constant stress and temperature, the "change-in-stress" technique[35] was used on selected specimens. The "change-in-temperature" method could not be used in the present study because of unduly long times to reach thermal equilibrium after a temperature change.

In order to minimize oxygen pick-up during testing the gage lengths were wrapped with Ta foil. However, this precaution was not sufficient to eliminate oxygen absorption during long-time tests.

The structures of crept specimens were examined by both optical and electron microscopy. An attempt was made to etch pit the crept specimens, but no technique was found which gave a convincing one-to-one correspondence between etch pits and dislocations. The technique that best revealed both the dislocation substructure and precipitate distributions was the following: (1) electropolish in a solution of 85 percent H_2SO_4, 15 percent HF maintained at room temperature using a Pt cathode and 10 volts dc and (2) etch by immersion or swabbing in a solution of 60 percent lactic acid, 20 percent HNO_3, 20 percent HF. Thinning foils for transmission electron microscopy was done by the jet indentation technique. Discs about 0.015 inch thick were chemically indented from both sides to a central thickness of ~0.003 inch using a solution of 60 percent HNO_4 and 40 percent HF. The specimens were then thinned electrolytically in a solution of 92.5 percent methanol, 2.5 percent HF, 5 percent H_2SO_4 maintained at -40 C. Thinning was stopped when a hole was visually observed in the central section of the disc.

RESULTS AND DISCUSSION

Cb-752

Creep Studies

Creep of the Cb-10W-2.5Zr alloy results in strain-time curves that are typical of metals that undergo dynamic strengthening during creep[30], e.g., strain aging or precipitation during deformation. Figure 27 illustrates the early stages of a creep test at 1000 C and 18,000 psi. A short primary region (Stage I) is followed by a region of markedly reduced creep rate (Stage II). The creep rate then rapidly accelerates during Stage III. The initial portion of Stage III is not associated with necking, since visual

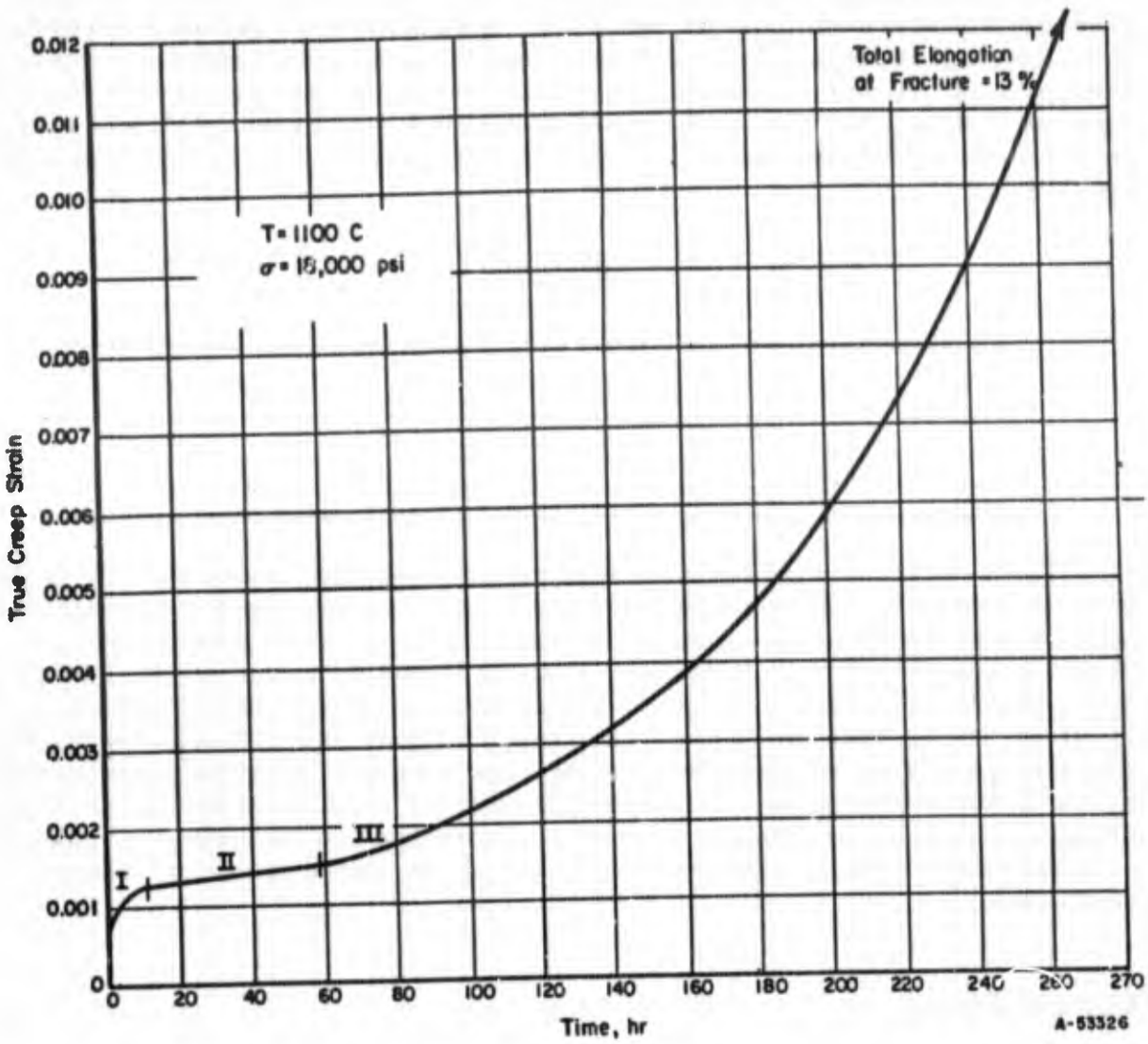

FIGURE 27. EARLY STAGES OF CREEP OF Cb-752 AT 1100 C AND 18,000 PSI

observations showed that necking does not occur until ~10 to 15 percent elongation. The rapid acceleration of the creep rate during Stage III may be associated with some dislocation multiplication process, as described by Gilman[36]. The reduction in the creep rate at the start of Stage II was even more marked in specimens tested at 800 C, i.e., tensile tests indicate that dynamic strengthening is most pronounced at this temperature (see Figure 7).

The stress dependence of the minimum creep rate at 800 C is shown in Figure 28. These results show that $\dot{\epsilon}_{min} \propto \sigma^n$, where the exponent $n = 4.8$. Several "change-in-stress" tests gave similar stress exponents (see Table 4), and a creep curve typical of this type of test is shown in Figure 29. In each case the stress changes were made during Stage II of the creep curve. A stress exponent of 4.4-4.9 agrees well with previous results of McCoy[37], who obtained $n = 4.8$-4.9 for a Cb-1Zr alloy creep tested at 982 and 1204 C.

TABLE 4. STRESS EXPONENTS CALCULATED FROM STRESS-CHANGE TESTS ON Cb-752

T, C	σ_1, psi	$\dot{\epsilon}_1$, per sec	σ_2, psi	$\dot{\epsilon}_2$, per sec	n
800	40,000	8.30×10^{-10}	42,000	1.03×10^{-9}	4.4
1100	16,000	1.53×10^{-9}	18,000	2.64×10^{-9}	4.6

The temperature dependence of the minimum creep rate, from 1000-1175 C, is shown in Figure 30. The relation between the minimum creep rate and temperature is $\dot{\epsilon}_{min} \propto \exp-(Q_c/RT)$, and the activation energy for creep was calculated to be $Q_c = 58$ kcal/mole at 22,000 psi. This value is in accord with the creep results of Gregory and Rowe[20] on a Cb-1Zr alloy. In the temperature range 1000-1125 C they measured Q_c values ranging from ~59-75 kcal/mole, with the higher values obtained for higher applied stresses. They suggested that pinning of jogged edge dislocations by Zr atoms inhibited climb, and the presence of interstitial atoms on the dislocations increased the binding energy of the Zr atoms to the jogs. It is possible that the same mechanism may be operative in Cb-752, but the present data are insufficient to justify any definite conclusions.

Structural Studies

It is particularly difficult to analyze the present results in terms of a rate-controlling mechanism. The situation is complicated by the fact that in addition to the normal recovery and dynamic strengthening processes, internal oxidation occurs, and in long-time tests a significant strengthening can occur as a result of formation of fine ZrO_2 precipitates. Thus, the minimum creep rate may be determined by dynamic strengthening caused by strain aging or precipitation on dislocations coupled with concurrent internal oxidation.

For example, in a 1000-hour test at 1000 C and 22,000 psi, the total oxygen content of the gage length was increased from 112 ppm O_2 to 870 ppm O_2. Undoubtedly part of this oxygen combined with Zr to form ZrO_2 precipitates. In view of the results of previous work on ultrahigh vacuum creep of Cb alloys it is not surprising that considerable

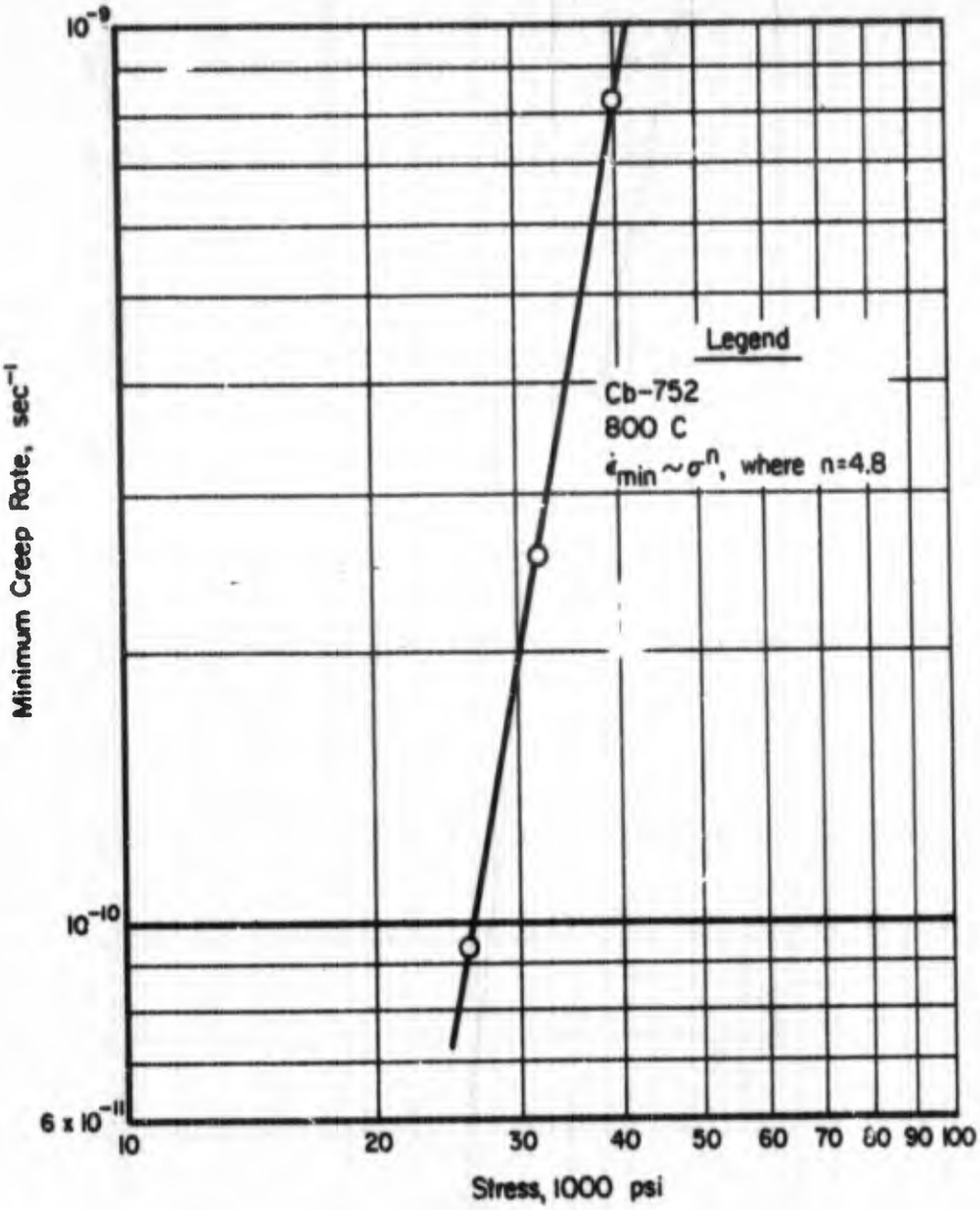

FIGURE 28. STRESS DEPENDENCE OF THE MINIMUM CREEP RATE OF Cb-752 AT 800 C ,

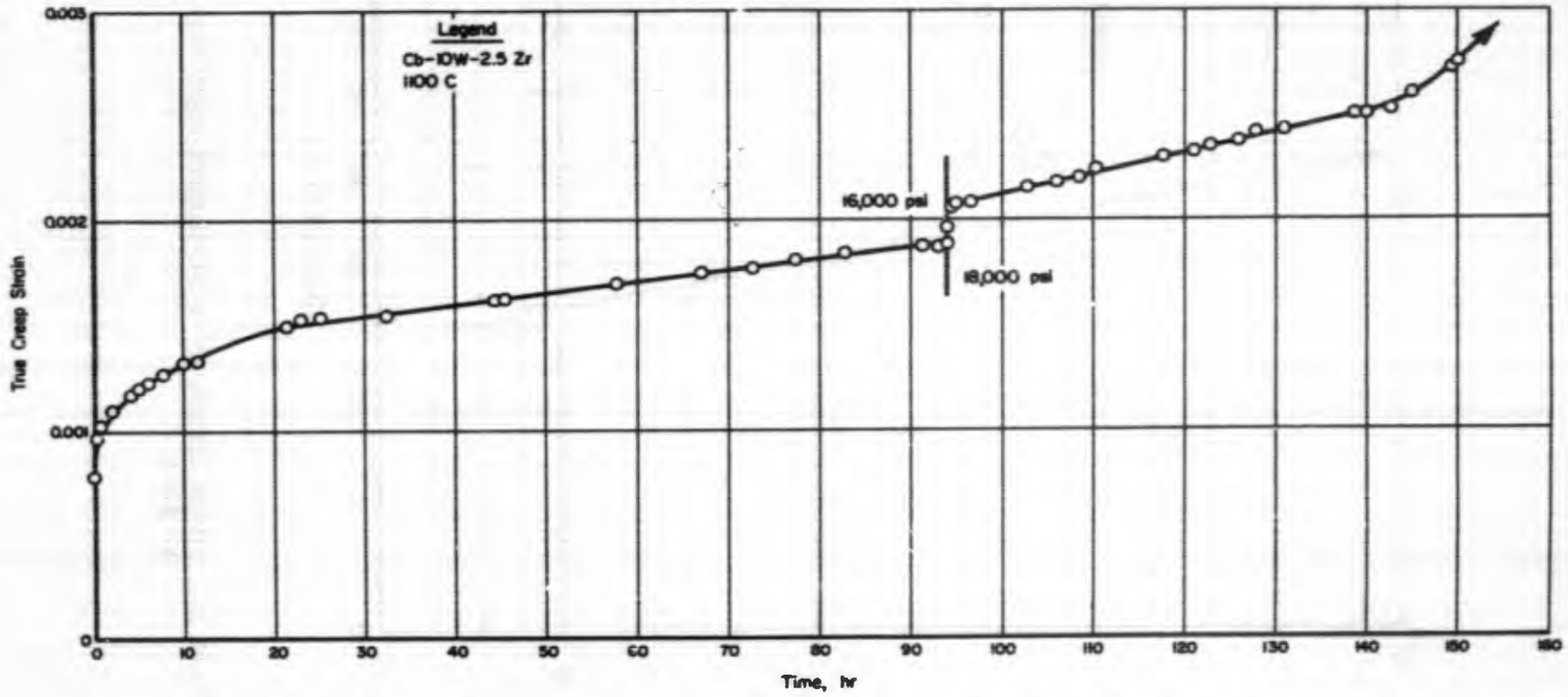

FIGURE 29. CHANGE-IN-STRESS CREEP TEST FOR Cb-752 AT 1100 C

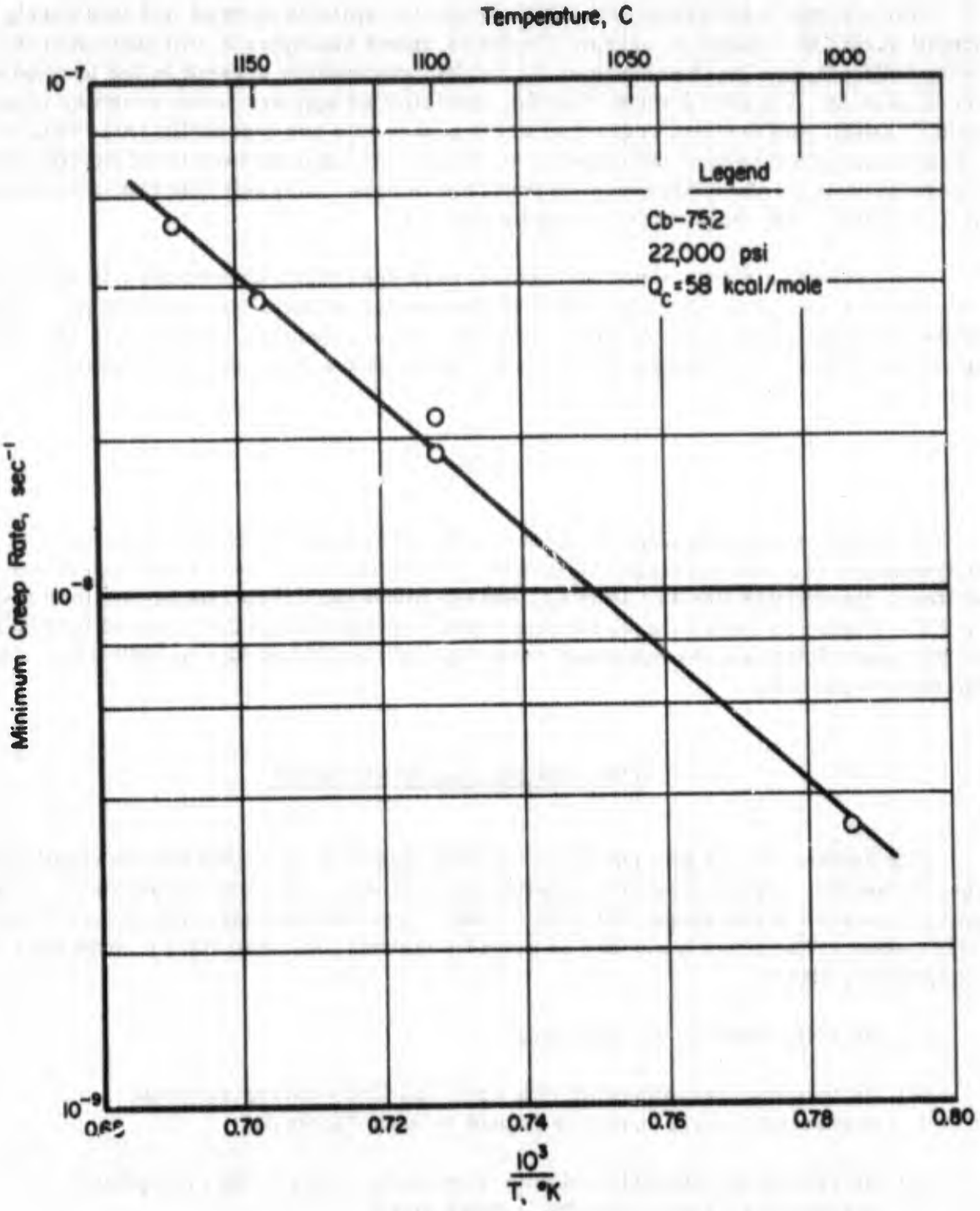

FIGURE 30. TEMPERATURE DEPENDENCE OF THE MINIMUM CREEP RATE OF Cb-752 TESTED AT 22,000 PSI

oxygen pickup occurred during the present tests. Titran and Hall[39] even found slight oxygen contamination (20-100 ppm O_2 increase) in long-time creep tests of various Cb alloys at vacuums of 10^{-8} to 10^{-9} torr.

Microscopic examination of crept specimens typically showed that fine precipitates formed during the course of creep. Figure 31 shows examples of this phenomenon. This precipitation is on a finer scale than the banded precipitates present in the uncrept alloy (see Figure 1). Figure 31 shows that the precipitation appears to be irregular from grain to grain, and denuded regions at grain boundaries are frequently noted (Figure 31a). In addition, a substructure develops within the grains, and appears to be heavily locked by precipitation on the subboundaries (see Figure 31b). It is felt that this precipitation arises largely from the internal oxidation process.

Transmission electron microscopy of crept specimens showed the fine particles in more detail (see Figure 32). The precipitates were not identified in this study. However, similar investigations by Rowcliffe, et al.[38], on an internally oxidized Cb-1W-1Zr alloy revealed that such precipitates could be monoclinic zirconium oxide (αZrO_2).

Cb-10W Alloy

Selected creep tests were made on the Cb-10W alloy at temperatures greater than its dynamic strengthening range (~200-500 C, see Figure 8). At a given stress and temperature, the rupture life was shorter, and the minimum creep rate higher than for Cb-752. Figure 33 shows the significant creep-strengthening effect caused by Zr, e.g., at 800 C and 32,000 psi the minimum creep rate of Cb-10W-2.5Zr is 3600 times less than that of Cb-10W.

The Strengthening Effects of Zr

The addition of 2.5 percent Zr to Cb-10W significantly increases the tensile and creep strengths. The degree of strengthening depends on the test temperature, being most pronounced in the range ~700-900 C where dynamic strengthening occurs in the Cb-752 alloy. There are a number of possible mechanisms whereby Zr could exert this strengthening effect:

(1) By solid solution strengthening.

(2) By forming precipitates of (Cb, Zr)C and ZrO_2 during material processing, e.g., compare Figure 1a with Figure 1b.

(3) By promoting internal oxidation (formation of fine ZrO_2 precipitates) during the course of long-time creep tests.

(4) By raising the temperature range where dynamic strengthening is operative. This could be due to:

400X a.

400X b.

FIGURE 31. MICROSTRUCTURE OF Cb-752 SPECIMEN CREPT AT 1100 C AND 15,000 PSI

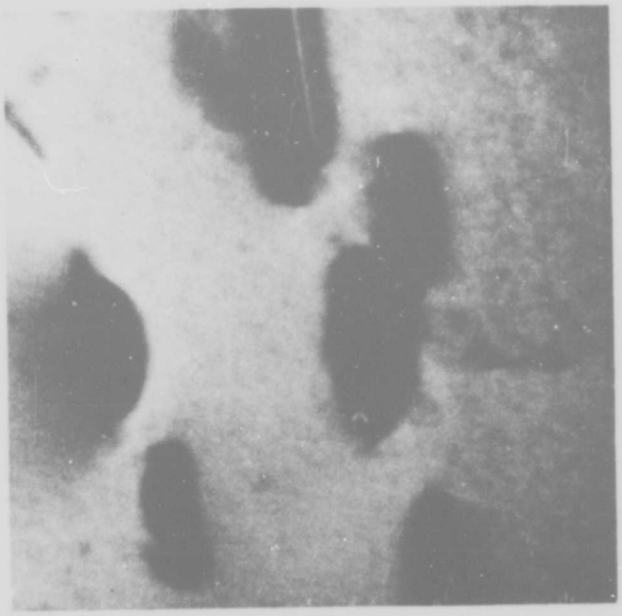

43,000X E1860

FIGURE 32. TRANSMISSION MICROGRAPH OF Cb-752 CREPT AT 1100 C AND 15,000 PSI, SHOWING FINE PRECIPITATES

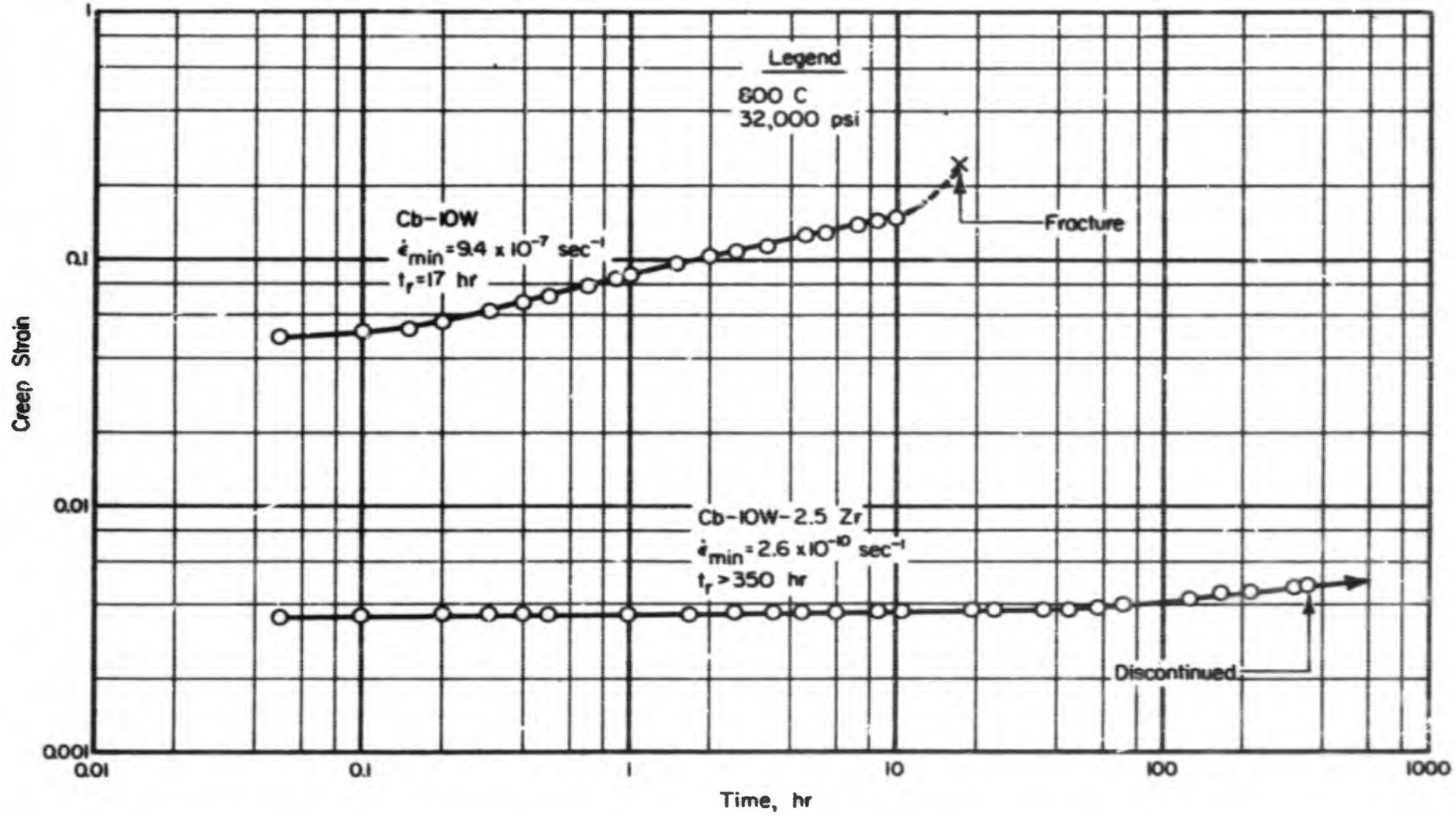

FIGURE 33. A COMPARISON OF THE CREEP BEHAVIOR OF Cb-10W AND Cb-10W-2.5Zr

(a) Strain-induced dyr amic precipitation on dislocations

(b) Zr modifying the diffusivity of interstitials such as oxygen, i.e., an alloy strain-aging effect.

(5) By forming Zr-O clusters in the matrix that impede dislocation climb and glide.

It is difficult to separate the effects of mechanisms (1) and (2). However, a rough estimate of the combined strengthening effects of (1) and (2) is possible from the room-temperature yield-strength values (see Figures 7 and 8). The 0.2 percent offset yield strength of Cb-10W-2.5Zr is ~60,000 psi, which is 12,000 psi higher than the corresponding value for Cb-10W. This strength improvement due to Zr is probably largely due to the combined effects of mechanisms (1) and (2).

Internal Oxidation

Figures 31 and 32 show that internal oxidation occurs during long-time vacuum creep tests of Cb-752. The formation of very fine ZrO_2 precipitates contributes to the creep strength by reducing the creep rate and prolonging the rupture life. The effect of internal oxidation on tensile and creep strengths of a Cb-1W-1Zr alloy has been discussed in more detail by Rowcliffe, et al.[38] They found that internal oxidation for 100 hours in a vacuum of 2×10^{-6} torr increased the room-temperature yield strength from ~30,000 psi to ~60,000 psi. The annealing treatment caused a fivefold increase in oxygen content, and resulted in the formation of fine coherent precipitates. These zones were not stable at 1100 and 1200 C, and they coarsened to αZrO_2 particles.

Even though the precipitates formed in Cb-Zr alloys are not completely stable at high temperatures, this method of strengthening offers considerable promise as a means of increasing the intermediate-temperature (~700-900 C) tensile and creep strength of Cb-Zr base alloys.

Dynamic Strengthening

In the temperature range ~600-950 C dynamic strengthening contributes significantly to the strength improvement of Cb-10W-2.5Zr over Cb-10W. This is best noted in tensile tests where the complicating effects of internal oxidation are minimal.

The influence of Zr on dynamic strengthening in Cb alloys is directly analogous to the effect of Mn on Fe-N and Fe-C alloys[40-44]. For example, in Fe-C-Mn and FeN-Mn alloys Baird and Jamison[44] noted tensile-strength peaks ~200 C higher than the normal Fe-C and Fe-N strain-aging peaks. Hopkin[41] also demonstrated that Mn and N together in pure iron are required to produce a marked increase in creep strength at 450 C, i.e., this is ~200 C higher than the normal nitrogen strain-aging peak in Fe. They suggested that clusters of Mn and N atoms form and impede dislocation movement. They also demonstrated that fine precipitates formed during creep, but they felt that this means of strengthening was less important than the Mn-N clustering. The Mn-N effect on creep could also be due to some form of dynamic alloy strain aging – where Mn may decrease the diffusion rate of N, thereby raising the effective strain-aging-temperature range. The high-temperature dynamic strengthening effects in the Cb-10W-2.5Zr alloy

can be discussed in terms of the same mechanisms, although the present study does not allow a single mechanism to be selected as most predominant. It is possible that several factors contribute to the Zr effect, including clustering of Zr and O atoms in solution as well as dynamic precipitation during tensile and creep deformation. There is evidence from internal friction studies in a Cb-1Zr alloy that a damping peak can be ascribed to a Zr-O interaction[45]. This was attributed to the diffusion of oxygen in the vicinity of Zr atoms. The Zr-O interaction could exert an alloy strain-aging effect or could cause strengthening by cluster formation. Dynamic precipitation on dislocations is quite possible also, but at present there is no direct evidence that this occurs in Cb-Zr alloys.

CONCLUSIONS

(1) Dynamic strengthening probably contributes to the higher creep strength of Cb-10W-2.5Zr (Cb-752) as compared with Cb-10W.

(2) The exact mechanism of dynamic strengthening is still uncertain. However, several reasonable suggestions are (a) the formation of Zr-O clusters which impede dislocation glide and climb, (b) dynamic precipitation on dislocations and in the matrix during deformation, and (c) an alloy strain-aging effect involving interaction of Zr and oxygen with moving dislocations.

(3) In long-time vacuum (10^{-6} torr) creep tests strengthening due to internal oxidation is superimposed on the normal dynamic strengthening process(es). This method of strengthening offers promise as a means of improving the intermediate-temperature (~700-900 C) creep and tensile strength of Cb-Zr alloys.

REFERENCES

(1) Gadd, J. D., "Design Data for Coated Columbium Alloys", TAPCO Report ER-5185, Contract No. NOw 62-0098c (January, 1963).

(2) Warmuth, D. B., "Design Data for Coated Columbium Alloys", TRW Report ER-5885, Contract No. NOw 63-0471c (April, 1964).

(3) Wurst, J. C., and Gerdeman, D., "Hot Bend Ductility of Columbium Base Alloys", University of Dayton Research Institute report prepared for 11th Refractory Composites Working Group Meeting (January, 1966).

(4) Elliott, R. P., Constitution of Binary Alloys, First Supplement, McGraw-Hill (1965), p 276.

(5) Metcalfe, A., and Dunning, J. S., "Interstitial Sink Effects in the Refractory Metals", Solar Report RDR 1392 on AF 33(615)-5233 (1966).

(6) Bewley, J. G., and Schussler, M., "Final Report on Process Development of Columbium (Cb752) Alloy", Union Carbide Corporation, Technical Report, AFML-TR-65-63 (March, 1965).

(7) Gadd, J. D., "Advancement of Protective Coating Systems for Columbium and Tantalum Alloys", TRW Technical Report, AFML-TR-65-203 (April, 1965).

(8) Lynch, J. F., et al., "Refractory Ceramics of Interest in Aerospace Structural Applications – A Materials Selection Handbook", ASD-TDR-63-4102 (1963); Supplement 1 (1964); Supplement 2 (1965).

(9) Bracco, D. J., Lublin, P., and Sama, L., "Identification of Microstructural Constituents and Chemical Concentration Profiles in Coated Refractory Metal Systems", Sylcor Division of General Telephone and Electronics Corp., Report AFML-TR-66-126 (May, 1966).

(10) Krafft, J. M., and Hahn, J. C., U. S. Patent No. 3,194,062, "Tension-Compression Testing Machine" (July 13, 1965).

(11) Wilcox, B. A., Gilbert, A., and Allen, B. C., "Intermediate Temperature Ductility and Strength of Tungsten and Molybdenum TZM", Battelle Report AFML-TR-66-89 (April, 1966).

(12) Doering, H., and Shahinian, P., "Brightness and Two-Color Pyrometry Applied to the Electron Beam Furnace ", NRL Report No. 6062 (December, 1963).

(13) Chang, W. H., "A Study of the Influence of Heat Treatment on Microstructure and Properties of Refractory Alloys", ASD-TDR-62-211 (April, 1962).

(14) Dyson, B. F., and Jones, R. B., J. Inst. Metals, 87, 340-342 (1958-1959).

(15) Wessel, E. T., France, L. L., and Begley, R. T., "The Flow and Fracture Characteristics of Electron-Beam-Melted Columbium", Columbium Metallurgy, Interscience (1961), pp 459-502.

(16) Cottrell, A. H., and Bilby, B. A., Proc. Roy. Soc. (London), A62, 49 (1949).

(17) Cochardt, A. H., Schoeck, G., and Wiedersich, H., Acta Met., 3, 533 (1955).

(18) Cottrell, A. H., Phil. Mag., 94, 829 (1953).

(19) Friedel, J., Les Dislocations, Gauthier Villors (1956), p 269.

(20) Gregory, D. P., and Rowe, G. H., "Mechanisms of Creep in Columbium and Columbium-1% Zirconium Alloy", Columbium Metallurgy, Interscience (1916), pp 309-341.

(21) Klopp, W. D., "Oxidation Behavior and Protective Coatings for Columbium and Columbium-Base Alloys", DMIC Report 123 (January 15, 1960).

(22) Timoshenko, S., Strength of Materials, 2nd Edition, Part 1, D. Van Nostrand Company, Inc. (1949), pp 217-219.

(23) Neshpor, V. S., and Reznichenko, M. I., "Investigating the Thermal Expansion of Some Silicides", Ogneupory, No. 3, 134-137 (March, 1963).

(24) Bartlett, R. W., "Investigation of Mechanisms for Oxidation Protection and Failure of Intermetallic Coatings for Refractory Metals", AARL Technical Report, ASD-TDR-63-753, Part III, Contract No. AF 33(657)-9170 (September, 1965).

(25) Metals Handbook Committee, Metals Handbook, 8th Edition, Vol 1, Properties and Selection of Metals, ASM (1961).

(26) Goldsmith, A., et al., Handbook of Thermophysical Properties of Solid Materials, Vol 1, Macmillan (1961).

(27) Beck, E. J., and Schwartzberg, F. R., "Determination of Mechanical and Thermophysical Properties of Refractory Metals", Martin Company Technical Report, AFML-TR-65-247 (July, 1965).

(28) Morey, G. W., The Properties of Glass, Reinhold (1938), Chapter XI.

(29) Wilcox, B. A., and Rosenfield, A. R., "On Serrated Yielding and Negative Strain Rate Sensitivity", to be published in Mat. Sci. and Engr.

(30) Cottrell, A. H., "Creep and Aging Effects in Solid Solutions", Creep and Fracture of Metals at High Temperature, Proc. NPL Symposium, Her Majesty's Stationery Office, London, 1956.

(31) Dumbleton, M. J., "Discontinuous Flow in Zinc Crystals and Its Relationship to Strain Aging", Proc. Phys. Soc., 67(B) (1954), pp 98-104.

(32) Glen, J., ASTM Spec. Tech. Pub. No. 128, 184 (1952).

(33) Borch, N. R., Shepard, L. A., and Dorn, J. E., "Activation Energies for Creep of an Alpha Solid Solution of Magnesium in Aluminum", Trans. ASM, 52, 494 (1960).

(34) Fullman, R. L., Carreker, R. P., and Fisher, J. C., AIME Trans., 197, 657 (1953).

(35) Dorn, J. E., Creep and Recovery, Am. Soc. Met. (1957), p 255.

(36) Gilman, J. J., J. Appl. Phys., 36, 2772 (1965).

(37) McCoy, H. E., Less, J., Common Met., 8, 20 (1965).

(38) Rowcliffe, D. J., Bonesteel, R. M., and Tietz, T. E., "Strengthening of N6-Zr Alloys by Internal Oxidation", paper presented at the Oxide Dispersion Strengthening Conf., Lake George, New York (June, 1966).

(39) Titran, R. H., and Hall, R. W., "Ultrahigh-Vacuum Creep Behavior of Columbium and Tantalum Alloys at 2000 and 2200 F for Times Greater Than 1000 Hours", NASA TM X-52130 (1965).

(40) Baird, J. D., and MacKenzie, C. R., J.I.S.I., 202, 427 (1964).

(41) Hopkin, L.M.T., J.I.S.I., 203, 583 (1965).

(42) Glen, J., J.I.S.I., 190, 114 (1958).

(43) Baird, J. D., "Strain Agency of Steel – A Critical Review", Iron and Steel Mist. (1963).

(44) Baird, J. D., and Jamison, A., "The Effect of Carbon, Nitrogen and Manganese on the High Temperature Tensile Properties of Iron", N.P.L. Conf. on The Relations Between Structure and Mechanical Properties of Metals and Alloys (1963).

(45) Bunn, P. M., Cummings, D. G., and Leavenworth, H. W., J. Appl. Phys., 33, 3009 (1962).

APPENDIX A

ESTIMATE OF OVERALL LONGITUDINAL STRESSES PRODUCED IN Cr-Ti-Si COATED Cb-752 AS A RESULT OF DIFFERENTIAL THERMAL CONTRACTION

A source of residual stresses in silicide-coated columbium alloys arises from differences in thermal expansion between coating and substrate. This stress state can be changed by (1) varying the specimen thickness and (2) altering the chemical composition of the coating by diffusion annealing. The maximum longitudinal stress can be estimated from an elastic analysis[22]. Consider a narrow, flat bar of thickness t_1, symmetrically coated on two opposite faces with materials having thicknesses defined as $t_2/2$ and $t_3/2$ for mathematical convenience (see Figure 34). With the following assumptions, the residual stress state can be calculated:

(1) The system is stress free at the coating temperature T_o. Should oxidation occur, it is assumed that stresses generated by the volume increase of the oxide are completely relieved by viscous flow of the resulting glass.

(2) The system is elastic.

(3) The differences in thermal-expansion coefficients $(\alpha_1 - \alpha_2)$ and $(\alpha_1 - \alpha_3)$ remain constant throughout the temperature interval, ΔT.

(4) Interfaces are discrete.

(5) The stress is uniform throughout the cross section. This is valid in the central portions, removed from edges where bond shear stresses and stresses normal to the bond are appreciable.

By balancing forces and maintaining continuity, the longitudinal stress in the substrate at $T = T_o - \Delta T$ is

$$\sigma_1 = \frac{E_1 \Delta T \left[E_2 t_2 (\alpha_1 - \alpha_2) + E_3 t_3 (\alpha_1 - \alpha_3) \right]}{E_1 t_1 + E_2 t_2 + E_3 t_3} \quad , \tag{3}$$

where E = Young's modulus at T. Similar relations can be written for stresses in the coating. If the bar were sufficiently wide, the stress would be increased by lateral restraint, and the effective modulus would be $E' = E/(1 - \mu)$, where μ = Poisson's ratio. Equation (3) would be altered by replacing E by E′ for each of three components and would result in ~50 percent increase in σ_1.

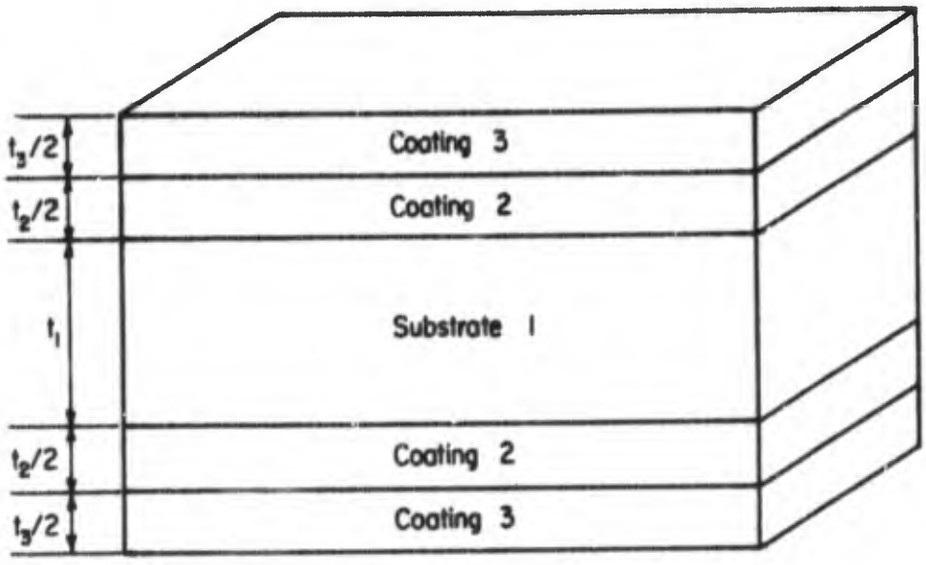

FIGURE 34. NARROW FLAT BAR OF SUBSTRATE SYMMETRICALLY COATED ON BOTH SIDES

Since the elastic modulus of pertinent metal silicides is ~45 x 10^6 psi from 25 to 1200 C[8], $E_2 \sim E_3$ and Equation (3) can be simplified to

$$\sigma_1 \sim \frac{E_1 \Delta T\ (\alpha_1 - \alpha_2) + \frac{t_3}{t_2}(\alpha_1 - \alpha_3)}{1 + t_3/t_2 + E_1 t_1 / E_2 t_2} \sim \frac{E_1 \Delta T (2\alpha_1 - \alpha_2 - \alpha_3)}{2 + E_1 t_1 / E_2 t_2} \quad . \tag{4}$$

The similarity on the right holds if $t_2 \simeq t_3$. Assuming $t_1 >> (t_2 + t_3)$, the resulting stresses in the coating layers are given approximately by

$$\sigma_2 \sim \frac{\sigma_1 t_1 (\alpha_2 - \alpha_1)}{t_2\ (\alpha_1 - \alpha_2) + \frac{t_3}{t_2}(\alpha_1 - \alpha_3)} \sim \frac{\sigma_1 t_1 (\alpha_2 - \alpha_1)}{t_2 (2\alpha_1 - \alpha_2 - \alpha_3)} \tag{5}$$

$$\sigma_3 \sim \frac{\sigma_1 t_1 (\alpha_3 - \alpha_1)}{t_3\ (\alpha_1 - \alpha_3) + \frac{t_2}{t_3}(\alpha_1 - \alpha_2)} \sim \frac{\sigma_1 t_1 (\alpha_3 - \alpha_1)}{t_3 (2\alpha_1 - \alpha_2 - \alpha_3)} \tag{6}$$

Estimates can be made of the physical-property data required for Equations (4) to (6). From a pertinent concentration profile in Figure 4, the composition and thickness of various layers can be estimated. Table 5 lists available thermal-expansion coefficients for pertinent silicides and oxides[8, 23, 24]. Differences in reported values indicate that thermal-expansion coefficients of silicides are not well established. The zirconium content of the coating is low and assumed negligible in this discussion. Using reported values for columbium, tungsten, and zirconium[25, 26], the expansion coefficient for the Cb-752 substrate was calculated from

$$\alpha = \alpha_{Cb} f_{Cb} + \alpha_W f_W + \alpha_{Zr} f_{Zr} \quad , \tag{7}$$

TABLE 5. SUMMARY OF REPORTED THERMAL-EXPANSION COEFFICIENTS OF INTEREST IN Cr-Ti-Si COATED COLUMBIUM ALLOYS

Component	Melting Temperature, C	Crystal Structure	Coefficient of Linear Thermal Expansion, 20-1200 C, 10^{-6}/C	Reference[a]
Cb	2435	Bcc	8.1	25,26
Cb-10W-2.5Zr	2500	Bcc	7.4, 8.1	6, 7
$CbSi_2$	2050	Hexagonal	11.0, 7.6	23,24
αCb_5Si_3	2000[b]	Tetragonal	6.4	24
WSi_2	2120	Tetragonal	7.6, 7.6, 7.5	8,23,24
W_5Si_3	2320	Tetragonal	5.1	24
$CrSi_2$	1540	Hexagonal	11.8, 14.6	8,23
Cr_5Si_3	1560	Tetragonal	11.0	23
$TiSi_2$	1500	Orthorhombic	10.6, 10.6	23,24
Ti_5Si_3	2120	Hexagonal	11.2, 17.0	23,24
SiO_2	1710	Amorphous	1	8
Cb_2O_5	1490	Orthorhombic	1.8	8
TiO_2	1800	Orthorhombic	9.3	8
Cr_2O_3	2330	Hexagonal	9.3	8

(a) Reference 23: Dilatometer measurements on hot-pressed 90 to 95 percent dense material containing 0.3 to 0.5 percent free silicon.

Reference 24: Dilatometer measurements on hot-pressed minus 325-mesh silicide powders; also X-ray measurements as minus 325-mesh powder and coatings produced by pyrolysis of silane vapor and by pack diffusion on refractory metals.

(b) Transformation temperature to β from.

where f = atomic fraction. In the temperature range 25 to 1200 C, the value of 7.9 x 10^{-6}/C agrees well with experimentally determined values[6, 27]. Relations similar to Equation (7) were used to calculate expansion coefficients of the diffusion zone, complex glass, and metal silicides probably to ±1 x 10^{-6}/C. Such calculations are reasonably valid for glasses[28] and presumed reliable for silicides. For simplification, layers having similar thermal expansions and elastic moduli were appropriately combined for analysis as indicated in Table 6. Young's modulus for the substrate is 15 to 13 x 10^6 psi from 25 to 1200 C[6], and that of pertinent oxides is ~30 x 10^6 psi[8]. Since the silicon was applied at 1120 C, this was chosen as the stress-free temperature.

The maximum longitudinal stresses calculated for as-coated 30- and 100-mil Cb-752 narrow sheet from Equations (4) to (6) are listed in Table 6. The relatively high thermal-expansion coefficients of the disilicide coating lead to high tensile stresses in the coating on the order of 100,000 psi at 25 C. The latter exceed reported bend strengths of ~50,000 psi, which in turn are slightly higher than corresponding tensile strengths[8]. In such a coating, one would expect and does encounter cracks extending to the thin subsilicide zone. Little yielding is expected in the substrate as the calculated compressive stresses are less than 30 percent of experimentally determined tensile yield stresses. Some relaxation in longitudinal stress would be expected because of cracks in the coating, but little from creep on cooling from the coating temperature. For example, if one assumes that the specimens were held an equivalent of 1 hour at 1000 C with a maximum stress of ~2000 psi resulting from differential thermal contraction, ~0.01 percent elastic strain would result. From creep data on Cb-752[6], a much higher stress of 10,000-15,000 psi is expected for 0.01 percent creep strain after 1 hour at 1000 C. On heating to 800 C, calculations indicate that the residual stresses drop to ~30 percent of the room-temperature values.

It should be noted that coating cracks introduce additional stresses because of violations of Assumption 5 in the analysis. A crack acts as an effective edge, thereby creating additional localized stresses. At the base of the crack, longitudinal stresses are zero, but bond shear stresses and normal stresses become appreciable. Although the latter can be estimated, further discussion is difficult because of lack of knowledge of important affecting parameters

The stress state after a diffusion anneal is different. The most important change is a thickening of the subsilicide zone, which has a relatively low thermal expansion coefficient. Ignoring the surface glass, calculations give large compressive stresses of ~70,000 psi in the subsilicide layer, large tensile stresses in the disilicide layer, and minor tensile stresses <10,000 psi in the substrate at 25 C. If the glass does not flow at all on cooling, calculations indicate the situation remains essentially the same except for a reduction in stress in the disilicide layer. As compressive fracture strengths of silicides are ~200,000 psi[8], no compressive failure would be expected in the subsilicide layer.

TABLE 6. ESTIMATES OF MAXIMUM LONGITUDINAL STRESSES IN Cb-752 SHEET COATED ON BOTH SIDES WITH Cr-Ti-Si

Layer[a]	Description[a]	Estimated Coefficient of Thermal Expansion, 25-1200 C, 10^{-6}/C	Nominal Young's Elastic Modulus, 25-1200 C, 10^6 psi	Nominal Thickness of Combined Layers, mils	Subscript in Elastic Analysis	Calculated Longitudinal Stress at 25 C[b], 1000 psi		Calculated Longitudinal Stress at 800 C[b], 1000 psi	
						30-Mil Sheet	100-Mil Sheet	30-Mil Sheet	100-Mil Sheet
			As Coated						
6	$(Cr,Ti,Cb,W)Si_2$	12	45	1.8	3	+135	+173	+39.4	+50.5
5	$(Cb,Cr,Ti,W)Si_2$	10	45	0.5	2	+67.6	+86.5	+19.7	+25.2
4	$(Cb,Ti,Cr,W)_2Si_2$	8	45						
3	$(Cb,Ti,Cr,W)_5Si_3$	8	45	30; 100	1	-18.5	-7.1	-5.4	-2.1
2	Diffusion Zone	8	45						
1	Cb-10W-2.5Zr Substrate	8	45						
			As Coated and Annealed 50 Hours at 1370 C in Air						
8	$SiO_2 + TiO_2$	3	30						
7	TiO_2	9	30	1	2	-61.5	-83.3	-18.0	-24.3
6	SiO_2	1	30			(0)	(0)	(0)	(0)
5	$TiO_2 \cdot Cb_2O_5 + SiO_2$	5	30						
4	$(Cb,Cr,Ti,W)Si_2$	9	45	1	3	+61.5 (+35.2)	+83.3 (+44.0)	+18.0 (+10.3)	+24.3 (+12.8)
3	$(Cb,Ti,Cr,W)_3Si_2$	6	45	1	2	-61.5 (-70.4)	-83.3 (-88.0)	-18.0 (-20.5)	-24.3 (-25.7)
2	$(Cb,Ti,Cr,W)_5Si_3$	6	45						
1	Cb-10W-2.5Zr Substrate	8	15	30; 100	1	+6.2 (+2.4)	+2.5 (+0.9)	+1.8 (+0.7)	+0.7 (+0.3)

(a) Deduced from Figure 1.

(b) Composite assumed to be stress-free at the coating temperature of 1120 C. + indicates tension, − indicates compression. Values in parenthesis assume that flow in the oxide layers completely relieves longitudinal stress in the oxide layers.

APPENDIX B

ANALYSIS AND HEAT TREATMENT OF UDIMET 700 TENSILE GRIPS

Udimet 700 alloy was obtained from Special Metals Corporation in 1/2- and 3/4-inch-diameter rod. The ladle analysis in weight percent was

Element	Weight Percent	Element	Weight Percent
Ni	Balance	Fe	0.15
Co	18.7	Zr	<0.05
Cr	15.1	Cu	<0.10
Al	4.49	Mn	<0.10
Ti	3.44	Si	<0.10
Mo	4.95	C	0.06
		B	0.014
		S	0.005

The wrought bar was air annealed according to the following schedule:

4 hr at 1180 C, air cool

4 hr at 1080 C, air cool

24 hr at 840 C, air cool

16 hr at 760 C, air cool .

APPENDIX C

TABULATED TENSILE DATA FOR PHASE 1

TABLE 7. TENSILE PROPERTIES OF UNCOATED 30-MIL Cb-752 SHEET TESTED IN VACUUM AT A STRAIN RATE OF 0.1 PER MINUTE

Temperature, C	0.2% Offset Yield Strength, 1000 psi	Ultimate Tensile Strength, 1000 psi	Fracture Stress, 1000 psi	% Elongation in 1 Inch	% Reduction in Area	Strain-Hardening Exponent	Other Observations
25	61.6	80.8	161	27	66	0.06	--
25	60.9	78.8	140	27	61	0.06	--
25	61.0	78.6	133	27	61	0.09	--
25	59.1	78.0	146	27	63	0.07	--
25	62.0	80.4	176	29	66	0.07	--
25	60.0	78.7	146	28	63	0.05	--
110	55.0	77.5	142	25	65	0.14	Yield point
215	47.8	67.6	139	19	61	0.09	--
295	47.6	66.9	150	24	73	0.09	Yield point
400	36.4	56.4	124	23	73	0.13	Yield point
500	33.0	55.1	164	23	79	0.15	Yield point
600	30.3	51.5	132	15	73	0.17	Yield point Serrations?
650	23.2	47.2	119	16	71	0.18	Serrations
700	27.1	49.5	128	17	77	0.17	Serrations
750	29.3	51.5	113	17	69	0.16	Serrations
795	30.2	52.8	112	16	70	0.18	Serrations
850	27.6	50.9	99	17	62	0.20	Serrations
890	27.6	51.4	99	16	66	0.20	Serrations
950	26.9	48.2	79	18	57	0.20	Serrations
1000	28.7	45.6	86	23	58	0.17	--
1095	25.5	37.1	63	33	55	0.13	--
1195	25.4	33.1	44	47	53	0.08	--
1395	20.7	22.7	23	98	87	0.04	--

TABLE 8. TENSILE PROPERTIES OF UNCOATED 100-MIL Cb-752 SHEET TESTED IN VACUUM AT A STRAIN RATE OF 0.1 PER MINUTE

Temperature, C	0.2% Offset Yield Strength, 1000 psi	Ultimate Tensile Strength, 1000 psi	Fracture Stress, 1000 psi	% Elongation in 1 Inch	% Reduction In Area	Strain-Hardening Exponent	Other Observations
25	58.0 (a)	74.1	152	30	69	0.05	--
25	56.7 (b)	73.1	187	31	75	0.05	--
310	47.2	67.5	167	28	76	0.08	Yield point
600	27.5	47.0	128	22	77	0.17	Yield point? Serrations
660	28.4	47.9	131	22	71	0.17	Yield point? Serrations
710	27.9	49.4	130	20	74	0.18	Serrations
750	26.6	47.8	125	20	73	0.19	Serrations
800	27.4	49.8	129	19	72	0.20	Serrations
850	26.7	48.8	126	20	72	0.19	Serrations
900	26.4	47.9	106	21	69	0.20	Serrations
940	26.4	46.6	109	20	69	0.20	--
1000	26.2	44.0	96	27	69	0.19	--
1100	24.5	37.0	70	30	66	0.16	--
1200	24.5	33.6	51	37	65	0.13	--

(a) Specimen axis transverse to rolling direction.
(b) Specimen axis parallel to rolling direction.

TABLE 9. TENSILE PROPERTIES OF UNCOATED 30-MIL Cb-10W SHEET TESTED IN VACUUM AT A STRAIN RATE OF 0.1 PER MINUTE

Temperature, C	0.2% Offset Yield Strength, 1000 psi	Ultimate Tensile Strength, 1000 psi	Fracture Stress, 1000 psi	% Elongation in 1 Inch	% Reduction in Area	Strain-Hardening Exponent	Other Observations
25	48.0	57.6	171	27	74	0.04	Yield point
25	47.4	58.1	158	20	74	0.04	Yield point
25	47.5	57.6	148	20	74	0.04	Yield point
200	47.4	61.3	188	26	79	0.08	Yield point
300	48.0	60.1	179	18	75	0.07	Yield point
400	36.6	60.3	137	18	71	0.22	Yield point Serrations
500	32.5	60.1	121	13.5	66	0.20	Yield point Serrations ?
600	26.4	48.0	124	12	69	0.20	Yield point
650	23.4	41.4	118	13	74	0.23	Yield point
700	25.6	45.0	128	15	77	0.23	--
750	22.1	38.2	125	18	78	0.23	--
800	16.2	24.8	124	25	88	0.23	--
850	18.3	28.2	120	25	87	0.18	--
900	13.1	19.1	125	27	90	0.14	--
950	12.7	18.0	136	30	92	0.15	--
1000	10.5	14.9	154	23	95	0.14	--
1020	13.6	19.6	162	31	95	0.16	--
1100	11.9	15.4	154	18	95	0.11	--
1200	13.8	16.9	154	23	95	0.09	--

TABLE 10. SUBSTRATE TENSILE PROPERTIES OF Cr-Ti-Si COATED 30-MIL Cb-752 SHEET TESTED IN AIR AT A STRAIN RATE OF 0.1 PER MINUTE

Temperature, C	0.2% Offset Yield Strength, 1000 psi	Ultimate Tensile Strength, 1000 psi	% Elongation in 1 Inch	% Reduction in Area	Strain-Hardening Exponent
25	70.5	73.8	0.3	0.3	--
25	66.0	71.0	0.4	0.4	--
100	58.1	76.4	8.6	8.6	0.10
205	48.2	68.1	18	64	0.13
300	43.0	65.6	14	56	0.19
410	37.7	60.1	12	52	0.17
500	36.8	60.4	9	41	0.19
595	32.6	55.6	6.6	24	0.18
600	36.5(a)	57.1	5.8	5.8	0.16
650	35.0	51.5	5.5	15	0.15
700	34.3(a)	43.7	2.5	2.5	0.18
705	35.2	49.5	2.4	2.4	0.16
755	36.2	47.4	2.1	2.1	0.13
800	39.5(a)	44.9	1.3	1.3	0.08
810	32.6	41.7	1.3	1.3	0.08
850	34.8	43.7	1.1	1.1	0.10
900	37.1	45.9	1.1	1.1	0.11
910	33.3	43.1	1.0	1.0	0.09
950	32.8(a)	39.2	0.7	0.7	0.13
950	--	45.6	1.5	1.5	--
1010	33.3	46.2	2.0	2.0	0.16
1110	31.2	45.0	4.8	4.8	0.14
1200	25.5	39.3	14	16	0.15

(a) As coated and annealed in air 50 hr 1370 C.

TABLE 11. SUBSTRATE TENSILE PROPERTIES OF Cr-Ti-Si COATED 100-MIL Cb-752 SHEET TESTED IN AIR AT A STRAIN RATE OF 0.1 PER MINUTE

Temperature, C	0.2% Offset Yield Strength, 1000 psi	Ultimate Tensile Strength, 1000 psi	% Elongation in 1 Inch	% Reduction in Area	Strain-Hardening Exponent
25	64.9	64.9	0.2	0.2	--
190	47.1	64.0	23	81	0.08
400	35.3	53.1	24	81	0.15
600	29.4[a]	48.4	12	40	0.18
610	30.7	49.3	15	41	0.17
650	31.7	49.5	11	25	0.16
710	29.5	45.5	10	20	0.17
740	30.1	45.4	9	14	0.17
800	30.2[a]	43.5	3.2	3.2	0.17
810	28.1	39.7	2.7	2.7	0.17
850	29.3	41.4	2.9	2.9	0.17
900	28.9	43.1	2.8	2.8	0.16
950	29.9	44.4	4.6	4.6	0.16
1010	27.5	40.8	6.2	6.2	0.16
1095	~22.9[b]	39.1	14	18	--
1115	~23.5[b]	>36.1	>4	>4	--
1200	~22.1[b]	>32.5	>7	>7	--

(a) As coated and annealed in air 50 hr 1370 C.

(b) Pin or grip failure.

TABLE 12. SUBSTRATE TENSILE PROPERTIES OF Cb-752 SHEET TESTED IN AIR AT A STRAIN RATE OF 100 PER MINUTE

Substrate Thickness, mils	Temperature, C	0.2% Yield Strength, 1000 psi	Ultimate Tensile Strength, 1000 psi	% Elongation in 1 Inch	% Reduction in Area	Strain-Hardening Exponent
			Uncoated			
30	25	79.6	90.1	22	73	0.04
30	25	84.1	89.5	23	73	0.03
100	25	--	--	27	70	--
100	25	77.3	87.6	28	73	0.03
			Cr-Ti-Si Coated			
100	300	--	--	24	83	--
100	600	40.8	54.6	25	82	0.11
100	910	31.3	45.0	18	75	0.16
100	1000	--	--	17	71	--
100	1015	--	--	17	73	--
30	950	37.7	55.9	8	56	0.19

TABLE 13. SUBSTRATE TENSILE PROPERTIES OF Cr-Ti-Si COATED Cb-752 AND Cb-10W TESTED IN VACUUM AT A STRAIN RATE OF 0.1 PER MINUTE

Temperature, C	0.2% Offset Yield Strength, 1000 psi	Ultimate Tensile Strength, 1000 psi	Fracture Stress, 1000 psi	% Elongation in 1 Inch	% Reduction in Area	Strain-Hardening Exponent	Other Observations
			30-Mil Cb-752 Sheet				
600	33.3	56.0	86	10	61	0.20	Serrations
800	36.4	61.8	86	7.6	48	0.21	Serrations
810	35.5	58.1	76	7.4	48	0.20	Serrations
900	34.0	57.8	70	9	45	0.21	Serrations
900	35.7	60.5	69	7.8	37	0.20	Serrations
1000	34.3	54.5	55	11	17	0.17	--
1100	34.7	46.5	48	20	27	0.12	--
1200	29.8	37.7	38	22	28	0.09	--
1300	25.8	31.9	32	32	40	0.10	--
			100-Mil Cb-752 Sheet				
900	29.3	49.6	103	17	69	0.19	Serrations
			30-Mil Cb-10W Sheet				
500	19.4	34.6	79	15	41	0.23	--
			30-Mil Cb-10W Sheet, Coating Removed				
500	16.2	28.3	132	31	86	0.23	--
800	11.0	20.4	138	34	86	0.25	--

TABLE 14. SUBSTRATE TENSILE PROPERTIES OF Cr-Ti-Si COATED 30-MIL Cb-10W SHEET TESTED IN AIR AT A STRAIN RATE OF 0.1 PER MINUTE

Temperature, C	0.2% Offset Yield Strength, 1000 psi	Ultimate Tensile Strength, 1000 psi	% Elongation in 1 Inch	% Reduction in Area	Strain-Hardening Exponent
25	40.5	59.0	19	61	0.12
25	41.4	59.4	17	59	0.12
100	34.2	53.1	16	63	0.15
195	27.6	45.6	18	59	0.19
300	23.3	40.5	16	66	0.20
400	18.8	34.0	17	40	0.24
500	17.4	30.2	11	15	0.24
600	17.7	26.9	9	9	0.16
650	16.6	24.9	6.2	6.2	0.16
700	16.5	23.4	5.1	5.1	0.16
750	14.8	21.7	3.8	3.8	0.18
800	16.6	21.0	3.2	3.2	0.13
850	15.9	21.0	2.7	2.7	0.14
900	15.1	20.0	1.9	1.9	0.14
950	14.1	19.6	2.5	2.5	0.13
1000	14.6	19.2	2.3	2.3	0.12
1050	14.0	19.6	4.7	4.7	0.11
1100	13.7	19.8	12	15	0.10

TABLE 15. SUBSTRATE TENSILE PROPERTIES OF Ag-Si-Al-Mo COATED Cb-752 SHEET TESTED IN AIR AT A STRAIN RATE OF 0.1 PER MINUTE

Temperature, C	0.2% Offset Yield Strength, 1000 psi	Ultimate Tensile Strength, 1000 psi	% Elongation in 1 Inch	% Reduction in Area	Strain-Hardening Exponent
		30-Mil Sheet			
25	72.5	87.6	6.5	6.5	0.07
200	54.6	77.1	12	37	0.12
400	39.2	65.0	10	22	0.16
600	35.7	54.5	5.6	15	0.19
700	33.4	49.0	2.4	2.4	0.17
750	31.4	48.1	2.0	2.0	0.22
800	34.2	56.7	4.6	4.6	0.19
800(a)	32.1	56.1	7.6	7.6	0.21
900	31.4	56.9	7.5	7.5	0.22
900(b)	29.7	53.9	5.9	5.9	0.22
900(a)	34.2	57.0	3.4	3.4	0.20
1000	29.8	51.4	12	20	0.20
1100	29.3	42.6	9	17	0.13
		100-Mil Sheet			
900	28.5	52.7	11	21	0.21

(a) As coated and annealed in situ 4 hours 1100 C, then cooled to test temperature.
(b) As coated and annealed in situ 1 hour 1100 C, then cooled to test temperature.

Unclassified

Security Classification

DOCUMENT CONTROL DATA - R&D

(Security classification of title, body of abstract and indexing annotation must be entered when the overall report is classified)

1. ORIGINATING ACTIVITY (Corporate author) Battelle Memorial Institute Columbus Laboratories	2a. REPORT SECURITY CLASSIFICATION Unclassified 2b. GROUP

3. REPORT TITLE Elevated Temperature Ductility Minima and Creep Strengthening of Coated and Uncoated Columbium Alloys

4. DESCRIPTIVE NOTES (Type of report and inclusive dates)
Final Report, from 1 Sept 65 to 30 Aug 66

5. AUTHOR(S) (Last name, first name, initial)
Allen, B. C., Bartlett, E. S., and Wilcox, B. A.

6. REPORT DATE	7a. TOTAL NO. OF PAGES	7b. NO. OF REFS
Feb. 1967	73	45

8a. CONTRACT OR GRANT NO.	9a. ORIGINATOR'S REPORT NUMBER(S)
b. PROJECT NO.	AFML-TR-66-89 Part II
c.	9b. OTHER REPORT NO(S) (Any other numbers that may be assigned this report)
d.	

10. AVAILABILITY/LIMITATION NOTICES
Qualified requesters may obtain copies of this report from DDC.

11. SUPPLEMENTARY NOTES	12. SPONSORING MILITARY ACTIVITY
	Air Force Materials Laboratory WPAFB, Ohio

13. ABSTRACT

In Phase 1 an investigation was made of factors affecting the tensile ductility minimum behavior of coated columbium alloys in air in the intermediate temperature range 700-1100 C. In the case of TRW Cr-Ti-Si coated Cb-10W and Cb-10W-2.5Zr (Cb-752 Alloy), contamination and embrittlement by air at the base of coating cracks is the major factor responsible for loss of ductility. Apparent mechanical interaction between coating and substrate plays a smaller role, but becomes more important with decreasing substrate thickness. The presence of zirconium and dynamic strengthening of the substrate have relatively little effect on ductility.

A study of dynamic strengthening during creep of Cb-10W-2.5Zr and Cb-10W was the objective of Phase 2. All creep testing was done in a vacuum of $\sim 10^{-6}$ torr and under constant stress conditions. The temperature range of interest was ~800-1200 C. In long-time creep tests, the usual dynamic strengthening process in the Cb-10W-2.5Zr alloy was complicated by additional hardening due to internal oxidation. The Cb-10W-2.5Zr alloy was considerably stronger in creep than Cb-10W. The possible strengthening effects of Zr are discussed.

This abstract is subject to special export controls and each transmittal to foreign governments or foreign nationals may be made only with prior approval of the Metals and Ceramics Division, MAMP, Air Force Materials Laboratory, Wright-Patterson Air Force Base, Ohio, 45433.

DD FORM 1 JAN 64 1473

Unclassified

Security Classification

14. KEY WORDS	LINK A		LINK B		LINK C	
	ROLE	WT	ROLE	WT	ROLE	WT
Cb alloys (Cb-10W-2.5Zr, Cb-10W) Coatings Creep Ductility Minima Strength						

INSTRUCTIONS

1. ORIGINATING ACTIVITY: Enter the name and address of the contractor, subcontractor, grantee, Department of Defense activity or other organization *(corporate author)* issuing the report.

2a. REPORT SECURITY CLASSIFICATION: Enter the overall security classification of the report. Indicate whether "Restricted Data" is included. Marking is to be in accordance with appropriate security regulations.

2b. GROUP: Automatic downgrading is specified in DoD Directive 5200.10 and Armed Forces Industrial Manual. Enter the group number. Also, when applicable, show that optional markings have been used for Group 3 and Group 4 as authorized.

3. REPORT TITLE: Enter the complete report title in all capital letters. Titles in all cases should be unclassified. If a meaningful title cannot be selected without classification, show title classification in all capitals in parenthesis immediately following the title.

4. DESCRIPTIVE NOTES: If appropriate, enter the type of report, e.g., interim, progress, summary, annual, or final. Give the inclusive dates when a specific reporting period is covered.

5. AUTHOR(S): Enter the name(s) of author(s) as shown on or in the report. Enter last name, first name, middle initial. If military, show rank and branch of service. The name of the principal author is an absolute minimum requirement.

6. REPORT DATE: Enter the date of the report as day, month, year, or month, year. If more than one date appears on the report, use date of publication.

7a. TOTAL NUMBER OF PAGES: The total page count should follow normal pagination procedures, i.e., enter the number of pages containing information.

7b. NUMBER OF REFERENCES: Enter the total number of references cited in the report.

8a. CONTRACT OR GRANT NUMBER: If appropriate, enter the applicable number of the contract or grant under which the report was written.

8b, 8c, & 8d. PROJECT NUMBER: Enter the appropriate military department identification, such as project number, subproject number, system numbers, task number, etc.

9a. ORIGINATOR'S REPORT NUMBER(S): Enter the official report number by which the document will be identified and controlled by the originating activity. This number must be unique to this report.

9b. OTHER REPORT NUMBER(S): If the report has been assigned any other report numbers *(either by the originator or by the sponsor)*, also enter this number(s).

10. AVAILABILITY/LIMITATION NOTICES: Enter any limitations on further dissemination of the report, other than those imposed by security classification, using standard statements such as:

(1) "Qualified requesters may obtain copies of this report from DDC."

(2) "Foreign announcement and dissemination of this report by DDC is not authorized."

(3) "U. S. Government agencies may obtain copies of this report directly from DDC. Other qualified DDC users shall request through _____."

(4) "U. S. military agencies may obtain copies of this report directly from DDC. Other qualified users shall request through _____."

(5) "All distribution of this report is controlled. Qualified DDC users shall request through _____."

If the report has been furnished to the Office of Technical Services, Department of Commerce, for sale to the public, indicate this fact and enter the price, if known.

11. SUPPLEMENTARY NOTES: Use for additional explanatory notes.

12. SPONSORING MILITARY ACTIVITY: Enter the name of the departmental project office or laboratory sponsoring *(paying for)* the research and development. Include address.

13. ABSTRACT: Enter an abstract giving a brief and factual summary of the document indicative of the report, even though it may also appear elsewhere in the body of the technical report. If additional space is required, a continuation sheet shall be attached.

It is highly desirable that the abstract of classified reports be unclassified. Each paragraph of the abstract shall end with an indication of the military security classification of the information in the paragraph, represented as *(TS), (S), (C), or (U)*.

There is no limitation on the length of the abstract. However, the suggested length is from 150 to 225 words.

14. KEY WORDS: Key words are technically meaningful terms or short phrases that characterize a report and may be used as index entries for cataloging the report. Key words must be selected so that no security classification is required. Identifiers, such as equipment model designation, trade name, military project code name, geographic location, may be used as key words but will be followed by an indication of technical context. The assignment of links, rules, and weights is optional.